PNNL-24705
RPT-DVZ-AFRI-031

Pacific Northwest
NATIONAL LABORATORY
Proudly Operated by Battelle Since 1965

Assessment of Hexavalent Chromium Natural Attenuation for the Hanford Site 100 Area

September 2015

MJ Truex
JE Szecsody
NP Qafoku
R Sahajpal
L Zhong
AR Lawter
BD Lee

U.S. DEPARTMENT OF
ENERGY

Prepared for the U.S. Department of Energy
under Contract DE-AC05-76RL01830

PACIFIC NORTHWEST NATIONAL LABORATORY
operated by
BATTELLE
for the
UNITED STATES DEPARTMENT OF ENERGY
under Contract DE-AC05-76RL01830

Printed in the United States of America

Available to DOE and DOE contractors from the
Office of Scientific and Technical Information,
P.O. Box 62, Oak Ridge, TN 37831-0062;
ph: (865) 576-8401
fax: (865) 576-5728
email: reports@adonis.osti.gov

Available to the public from the National Technical Information Service
5301 Shawnee Rd., Alexandria, VA 22312
ph: (800) 553-NTIS (6847)
email: orders@ntis.gov <http://www.ntis.gov/about/form.aspx>
Online ordering: http://www.ntis.gov

This document was printed on recycled paper.
(8/2010)

PNNL-24705
RPT-DVZ-AFRI-031

Assessment of Hexavalent Chromium Natural Attenuation for the Hanford Site 100 Area

MJ Truex
JE Szecsody
NP Qafoku
R Sahajpal
L Zhong
AR Lawter
BD Lee

September 2015

Prepared for
the U.S. Department of Energy
under Contract DE-AC05-76RL01830

Pacific Northwest National Laboratory
Richland, Washington 99352

Summary

Hexavalent chromium (Cr(VI)) plumes are present in the 100 Area at the Hanford Site. Remediation efforts are under way with objectives of restoring the groundwater to meet the drinking-water standard (48 µg/L) and protecting the Columbia River by ensuring that discharge of groundwater to the river is below the surface-water quality standard (10 µg/L). Current remedies include application of Pump-and-Treat (P&T) at the 100-D, 100-H, and 100-K Areas and Monitored Natural Attenuation (MNA) at the 100-F/IU Area. Remedy selection is still under way at the other 100 Areas. Additional information about the natural attenuation processes for Cr(VI) is important in all of these cases. In this study, laboratory experiments were conducted to demonstrate and quantify natural attenuation mechanisms using 100 Area sediments and groundwater conditions.

Multiple lines of evidence are used in an MNA evaluation to demonstrate the presence of attenuation mechanisms and evaluate whether attenuation will be sufficient to meet remedial action objectives (RAOs). For the Hanford 100-D, 100-H, and 100-K Area Cr(VI) plumes, P&T operations have and are continuing to perturb the plume behavior (as designed) such that plume behavior cannot be directly used to assess natural attenuation rates. At these and other 100 Areas, plume conditions are in transition because source remediation actions were recently completed. Thus, monitoring well and plume trends must be interpreted in light of these declining or terminated source flux conditions. Where P&T has not been applied, direct monitoring over time may be suitable to demonstrate attenuation of plumes. For instance, plumes at the 100-F/IU and 100-BC Areas can be monitored in this way to support MNA evaluation. However, at these areas and other areas with some form of plume perturbation, predictive modeling is an important tool for evaluating MNA and its ability to meet RAOs. To support predictive modeling, a technical basis for selection of appropriate fate and transport parameters is needed to configure the model and to support interpretation of modeling results.

A series of laboratory-scale measurements provide evidence of Cr(VI) reduction in the Hanford 100 Area sediments. Loss of Cr(VI) was observed in stop-flow soil column experiments loaded with anoxic groundwater containing 300 µg/L Cr(VI) for five different sediment samples, four from the Hanford 100 Area and one from the Hanford 200 East Area. The Cr(VI) reduction was also observed under conditions using oxic groundwater containing Cr(VI). The rate of Cr(VI) reduction under oxic conditions was slower, but still occurred. While dissolved oxygen did not completely suppress Cr(VI) reduction in these tests, treatment of the sediments with 1% hydrogen peroxide, expected to fully oxidize the sediments and kill microorganisms, did stop Cr(VI) reduction. These results suggest that the sediments have a reductive capacity and that the reductive capacity for Cr(VI) can be active in the presence of dissolved oxygen. In tests with the addition of biocides, the Cr(VI) reduction rate decreased by a factor of about 5. A test with the addition of 5 mg/L lactate as a substrate for biotic activity showed a minor increase in the Cr(VI) rate. Thus, it is likely that a combination of biotic and abiotic processes were contributing to the overall observed Cr(VI) reduction.

Information was collected about Cr(VI) co-precipitation with calcium carbonate to assess its relevance to attenuation away from source areas. These studies were conducted to extend information previously reported for co-precipitated materials in source areas. These results extend the data about Cr(VI) co-precipitation from the literature to lower aqueous-phase Cr(VI) concentrations. An experiment conducted with a 44 ppb Cr(VI) solution showed that more than 86% of the aqueous Cr(VI) was removed from solution and likely was incorporated into the calcium carbonate precipitates. At higher initial Cr(VI)

concentrations, a lower percentage of the supernatant concentration (13−27%), but greater total mass of Cr(VI), was incorporated into the calcium carbonate precipitates. These data showed that even at low initial Cr(VI) concentrations, a substantial amount of Cr(VI) can co-precipitate with calcium carbonate and this mechanism may be relevant for Cr(VI) within the plume, not just within a source area.

The information provided in this study describes attenuation mechanisms associated with 1) Cr(VI) reduction to functionally immobile Cr(III) that acts as a loss mechanism (e.g., like degradation), 2) co-precipitation of Cr(VI) with calcium carbonate materials of moderate solubility that act as a solubility-controlled partitioning interaction with respect to slowing Cr(VI) transport (e.g., within the plume especially at the distal portions), and 3) co-precipitation of Cr(VI) with calcium carbonate materials of moderate solubility that may provide a continuing source of Cr(VI) (e.g., for the tail of a plume or near former source areas). The Cr(VI) reduction observed in the laboratory is expected to be difficult to directly observe in the field because 1) it may be masked by Cr(VI) concentrations and transport in higher permeability zones that are preferentially sampled by monitoring wells and 2) sediment samples collected at locations farther from the source areas would be expected to have low concentrations of Cr(VI) and Cr(III). Because Cr(VI) has been observed to be robust in the 100 Area sediments included in this study, it is reasonable to consider reduction as one of the attenuation mechanisms that can be attributed to declining plume conditions. However, for several reasons, the reductive capacity and rates observed in the laboratory tests are likely be higher than what would be expected at field scale. The laboratory results show that there is some finite capacity for Cr(VI) reduction. This capacity would be expected to vary spatially in the aquifer and be highest in the fine-textured zones. In evaluating future plume behavior, available reductive capacity at the distal portions of the plume and within finer-textured sediment features would be most appropriate to consider. Laboratory results provided a rough estimate of the capacity that could be used to constrain the reductive attenuation element of an attenuation assessment.

Co-precipitation of Cr(VI) with calcium carbonate has several implications. Source zone implications of the co-precipitated Cr(VI) were evaluated in a recent field investigation report for the Hanford Site. At this site, high Cr(VI) concentrations have sustained a Cr(VI) plume for decades. Release of Cr(VI) from the vadose zone was initially identified as the likely source based on a conceptual model that considers Cr(VI) a mobile contaminant. However, the finding of elevated sediment-associated Cr(VI) in the periodically rewetted zone and aquifer beneath the vadose zone source area demonstrated that dissolution of solid-phase Cr(VI) precipitates can occur as a continuing source. This type of co-precipitation process may also occur throughout the plume. As shown herein, co-precipitation occurs at Cr(VI) concentrations at least as low as 44 µg/L (below the drinking-water standard). Thus, within the plume some Cr(VI) plume retardation may occur due to this process. The information in this report provides a basis for considering “sorptive” attenuation through a solubility-controlled partitioning interaction, but additional efforts would be needed to quantify the Cr(VI) retardation factor related to these interactions.

Under current site conditions, observing the effects of Cr(VI) reduction or co-precipitation with calcium carbonate at the field scale would be difficult for several reasons. Until recently, Cr(VI) sources were still feeding aquifer plumes and creating increasing/stable plumes. Under conditions where the source flux is much higher than the attenuation capacity, this type of attenuation would be masked by the added Cr(VI). For the Hanford 100-D, 100-H, and 100-K Areas, P&T-induced plume movement would tend to mask any reductive attenuation that is occurring, even though reduction may be contributing to quicker decline of the plume than if it were not active. However, monitoring observations for the 100-F/IU and 100-BC Areas may provide important data for examining plume decline and the contributions to attenuation by dispersion, sorption, precipitation, and reductive processes.

Acknowledgments

This document was prepared by the Deep Vadose Zone − Applied Field Research Initiative at Pacific Northwest National Laboratory. Funding for this work was provided by the U.S. Department of Energy (DOE) Richland Operations Office. The Pacific Northwest National Laboratory is operated by Battelle Memorial Institute for the DOE under Contract DE-AC05-76RL01830.

Acronyms and Abbreviations

cm/min	centimeter(s) per minute
DOE	U.S. Department of Energy
DVZ-AFRI	Deep Vadose Zone − Applied Field Research Initiative
Eh	oxidation-reduction potential
EMP	electron microprobe
EPA	U.S. Environmental Protection Agency
ERDF	Environmental Remediation Disposal Facility
ERT	electrical resistivity tomography
µg/L	microgram(s) per liter
g	gram(s)
h	hour(s)
HPLC	high-performance liquid chromatography
ICP-OES	inductively coupled plasma- optical emission spectrometer (spectroscopy)
in.	inch(es)
kg	kilogram(s)
M	moles per liter
mg	milligram(s)
mg/L	milligram(s) per liter
mL	milliliter(s)
mL/min	milliliter(s) per minute
mm	millimeter(s)
MNA	Monitored Natural Attenuation
P&T	Pump-and-Treat
pCi/g	picocurie(s) per gram
PNNL	Pacific Northwest National Laboratory
QA	quality assurance
RAO	remedial action objective
µS/cm	microsiemens per centimeter
wt%	weight percent
XRD	X-ray diffraction

Contents

Figures

Tables

1.0 Introduction

Hexavalent chromium (Cr(VI)) is a prevalent contaminant in the Hanford 100 Area and its proximity to the Columbia River drives the need for remediation to both drinking-water and surface-water–quality standards. Current remedies include application of Pump-and-Treat (P&T) at the 100-D, 100-H, and 100-K Areas and Monitored Natural Attenuation (MNA) at the 100-F/IU Area. Remedy selection is still under way at the other 100 Areas. Additional information about the natural attenuation processes for Cr(VI) is important in all of these cases. For P&T remedies, the natural attenuation information can be helpful in evaluating when it is appropriate to transition from P&T to a passive remediation approach for all or part of the P&T system. For the MNA remedy or for plumes for which a remedy has not yet been selected, the natural attenuation information provides additional support in assessing the viability and/or performance of MNA in meeting the remedial action objectives (RAOs). Several types of information can be applied to support an MNA remedy decision at a specific site (EPA 2007a, b). One element of the assessment is examination of attenuation mechanisms and rates. Scientific literature provides one resource for information about mechanisms relevant to Cr(VI) attenuation.

Abiotic reduction of Cr(VI) in groundwater under natural conditions is facilitated by multiple compounds found in soils and sediments (Qafoku et al. 2003; Dresel et al. 2008; Qafoku et al. 2011). Reduced chromium (Cr[III]) has low solubility under typical aquifer geochemical conditions (Qafoku et al. 2010; Zhong et al. 2009). The U.S. Environmental Protection Agency (EPA) technical protocol for MNA of inorganic contaminants provides a good review of relevant reductive processes. In summary, ferrous iron is an important reductant (Bidoglio et al. 1993; Eary and Rai 1989; Ilton et al. 1997; Kent et al. 1994; Patterson et al. 1997; White and Peterson 1996; Qafoku et al. 2007; Qafoku et al. 2009) and may be present in many forms in an aquifer. Soil organic matter may also promote Cr(VI) reduction directly or indirectly (Deng and Stone 1996a, b; Wittbrodt and Palmer 1996).

Multiple types of microorganisms can directly reduce Cr(VI). Microbial reduction of chromium is either a fortuitous reductive process or the chromium is reduced by the bacteria to decrease its toxicity to the bacteria. The ability to reduce Cr(VI) to Cr(III) is distributed among a wide variety of bacteria (e.g., Horitsu et al. 1987; Bopp and Ehrlich 1988; Ishibashi et al. 1990; Caccavo et al. 1992; Lovley and Phillips 1994; Alam et al. 2006). Reduction typically occurs under anaerobic conditions with a suitable substrate present to promote growth and/or metabolism of nitrate-, iron-, and sulfate-reducing bacteria. Chromate reduction can also occur under aerobic conditions during microbial growth (Horitsu et al. 1987; Bopp and Ehrlich 1988; Ishibashi et al. 1990). The rate and extent of chromate reduction is dependent on its concentration (i.e., toxicity to bacteria) and on the type of microbes present and the dominant microbial process occurring. Thus, the relative concentration of electron acceptors can be an important factor for direct reduction of chromium.

The capability to reduce structural Fe(III) in minerals has been established for a number of microbial species (Fredrickson and Gorby 1996). These bacteria have a broad spectrum of other metabolic capabilities. For instance, Desulfovibrio desulfuricans is a well-known sulfate-reducing bacterium, but can also use Fe(III), U(VI), and Cr(VI) as electron acceptors (Lovley and Phillips 1992, 1994). The Fe(III) in minerals such as amorphous and poorly crystalline iron (e.g., ferrihydrite) (Lovley 1991; Coleman et al. 1993; Lovley 1994) and crystalline iron oxides/hydroxides (e.g., hematite, goethite, and magnetite) (Arnold et al. 1988; DiChristina 1994; Kostka and Nealson 1995; Roden and Zachara 1996) can be microbially reduced and create the potential for indirect reduction of Cr(VI).

Once Cr(VI) is reduced to Cr(III), the Cr(III) compounds are expected to be functionally immobile and, relevant to attenuation, studies indicate that reduced chromium is resistant to reoxidation. Available information indicates that the rate of oxidation of Cr(III) to Cr(VI) by oxygen is slow to insignificant (Eary and Rai 1987). Manganese oxides are naturally occurring oxidants capable of oxidizing Cr(III) to Cr(VI). In addition, recent studies have shown that Cr(III) may be oxidized and released as aqueous Cr6+ via a coupled reaction with the participation of dissolved Mn2+ (Namgung et al. 2014), which may be present in some subsurface environments. However, although Cr(III) oxidation may occur under specific conditions (i.e., on manganese oxides or in the presence of dissolved Mn2+), a number of factors have been found that greatly limit the progress and rate of this reaction (Eary and Rai 1987; Fendorf et al. 1992; Fendorf et al. 1993). Thus, Cr(III) may be considered functionally stable and is not expected to reoxidize at a rate that would form Cr(VI) concentrations of concern.

Sorption to sediments can also be an important attenuation mechanism. Most information about Cr(VI) sorption in the general literature comes from studies with pure mineral phases (Griffin et al. 1977; Davis and Leckie 1980; Leckie et al. 1980). These studies suggest that Cr(VI) adsorbs strongly to gibbsite (α-Al2O3) and amorphous hydrated ferric oxide (Fe2O3·H2O (am)) at low to medium pH values (i.e., pH 2−7) and adsorbs weakly to silica (SiO2) at all but very low pH values. However, adsorption of Cr(VI) over a range of pH values onto four different environmental soil samples varied from essentially no adsorption to extensive adsorption (Zachara et al. 1989). A more recent study confirmed that chromate adsorption to sediment was not significant (Qafoku et al. 2009). These studies examined slightly alkaline and oxic conditions, which are predominant in the Hanford subsurface, for which chromium in the sediments was present as 1) a highly mobile fraction (over 95% of the total chromium); 2) a fraction with a slow and time-dependent release during leaching, and 3) a fraction that was immobile Cr(III). The presence of competing and, less commonly, complexing ions may significantly alter chromate adsorption. Although sulfate is adsorbed less strongly on amorphous hydrated ferric oxide than CrO42-, sulfate may compete for adsorption sites when present in higher concentrations (Leckie et al. 1980).

Sequestration of Cr(VI) may also occur under some conditions and be important as an attenuation mechanism. Cr(VI) has been shown to be associated with calcium carbonate precipitates. Evidence for Cr(VI) co-precipitation with calcium carbonate is presented by Hua et al. (2007). In a separate study, chromium co-precipitation with calcium carbonate was also shown to be present as Cr(VI) through x-ray absorption near edge structure analysis (Tang et al. 2007). The presence of Cr(VI) in the calcium carbonate distorted the crystal structure but is consistent with substitution into the carbonate sites. In these studies, the CrO42- ion would occupy the same sites in the precipitate with calcium as the CO32- ion (i.e., forming a CaCrO4 precipitate).

Hexavalent chromium may also occur in relatively insoluble solids such as barium chromate, which is a moderately low-solubility Cr(VI) solid. The solid solution between barium chromate and barium sulfate can be precipitated at low temperatures and has a lower solubility than the pure end member barium chromate and may control the aqueous concentration of Cr(VI) when sufficient barium and sulfate are present (Rai et al. 1989). In addition, unidentified Cr(VI) solids were found in the Hanford Site vadose zone beneath the S-SX high-level-waste tank farm; a fraction of the solid Cr(VI) was resistant to leaching (Zachara et al. 2004).

While information available in the literature describes Cr(VI) attenuation via biological and abiotic reduction, formation of precipitates, and sorption, specific data and direct evidence of chromium natural attenuation for the Hanford 100 Area are limited. In this study, laboratory experiments were conducted to demonstrate and quantify natural attenuation by reduction or precipitation mechanisms using 100 Area sediments and groundwater conditions. This work supports consideration of attenuation mechanisms that may be relevant to the Cr(VI) plumes in the Hanford Site 100 Areas.

2.0 Methods

Two types of investigations were conducted. One investigation focused on evaluating chromium attenuation in sediment samples, primarily studies of Cr(VI) reduction (Section 2.1). In addition, solid phases of Cr(VI) were investigated as potential continuing sources and with respect to formation of solid phases as an attenuation process (Section 2.2).

Investigation of environmental samples included Ringold Formation aquifer sediment samples (Table 1) retrieved from split-spoon sampling at four borehole locations beneath an ~80 ft deep excavation in the Hanford Site 100-D area (excavation 100-D-100) (CHPRC 2015). Cores were collected using a 61 cm long sediment sampler, which was hammered below the end of the drilled depth to collect intact sediment. The 61 cm long sampler contained four plastic liners (15.2 cm in length by 10.2 cm in diameter) that were sealed with plastic caps taped on each end (in an oxic environment) after collection. No effort was made to control the redox environment during collection, although the capping limited any change in moisture. Liners were stored at $4^{o}C$ in a dark environment to limit microbial growth. Additional grab samples of Hanford formation sediment (Table 1) were obtained from the vadose zone accessed at the sidewall of excavations 100-D-100 and 100-D-104 based on visual location of yellow sediment (presumed chromate contaminated) (CHPRC 2015). Chromium attenuation analyses were also conducted for sediments collected from a borehole in the Hanford Site 100-N area and for grab samples of Hanford formation sediment from the excavation of the Hanford Site Environmental Remediation Disposal Facility (ERDF) (Table 1). Previous mineralogical characterization of Hanford and Ringold Formation sediments shows predominant phases are quartz, microcline, plagioclase, pyroxenes, amphiboles, magnetite, micas, and calcite (1.91 ± 1.71 % Hanford formation, 0.68 ± 0.92% Ringold Formation; Xie et al. 2003). Iron extractions were used to quantify ferrous and ferric iron for sediments 5, 8, 10, 15, 16, and 18. The iron extractions were conducted in an anaerobic chamber and consisted of 1) 1 M $CaCl_2$, 2) 0.5 M HCl, 3) 0.25 M NH_2OH, 0.25 M HCl, 4) dithionite-citrate-bicarbonate, and 5) 5 M HCl, as described in Table 1. The quantity of aqueous ferrous and ferric iron from each extraction was measured using the ferrozine method (Gibbs 1976).

Table 1. Sediment location and physical characterization

Sediment Number	Source	Nominal Depth of Sample (m)	Fraction < 4 mm
1	100-D Area borehole C8955	8.13(a)	0.879
2	100-D Area borehole C8955	9.41(a)	0.405
3	100-D Area borehole C8954	3.07(a)	0.312
4	100-D Area borehole C8954	10.41(a)	0.287
5	100-D Area borehole C8953	3.05(a)	0.305
6	100-D Area borehole C8953	6.47(a)	0.285
7	100-D Area borehole C8953	9.94(a)	0.332
8	100-D Area borehole C8956	3.11(a)	0.750
9	100-D Area borehole C8954	4.76(a)	1.0
10	100-D Area borehole C8955	3.27(a)	0.416
11	100-D-30/104 sidewall 1(b)	NA	0.311
12	100-D-30/104 sidewall 2[a]	NA	0.226
13	100-D-100 sidewall 1(c)	NA	NA(d)
14	100-D Area borehole C8956	3.43(a)	0.766
15	100-D Area borehole C8956	5.18(a)	0.306
16	100-D Area borehole C8956	6.10(a)	0.287
17	100-D Area borehole C8956	3.28(a)	0.766
18	ERDF excavation sidewall	NA	1.0
19	100-N Area borehole C4955	14.6	0.464

NA = not applicable.

(a) Depth below the bottom of the ~24.4-m deep 100-D-100 excavation in the 100-D Area of the Hanford Site.

(b) Sample collected in the sidewall of the 100-D-30/104 excavation in the 100-D Area of the Hanford Site just above the water table (CHPRC 2015).

(c) Sample collected in the sidewall of the 100-D-100 excavation in the 100-D Area of the Hanford Site just above the water table (CHPRC 2015).

(d) Focused sample of yellow crystalline material.

2.1 Investigation of Reductive Hexavalent Chromium Attenuation

Batch Cr(VI)-reduction experiments were conducted at a high sediment/water ratio (average 4.24 g-sediment/mL-water) similar to field conditions. The experimental matrix is summarized in Table 2. Sediment from the liners selected for Cr(VI) reduction experiments (Table 2) were emptied and sieved to remove particles greater than 4 mm. The total liner sediment weight and all larger particles were retained for use in data analysis calculations. The field moisture content on the <4 mm fraction was also determined by wet and dry weights using a subsample. A subsample of the <4 mm fraction of the sediments were loaded into a 1.47 cm diameter by 53 cm long stainless-steel column with 2 µm Teflon end frits. The experimental procedure consisted of 1) anaerobic conditioning, 2) Cr(VI) loading, and 3) the Cr(VI) reduction experiment. The anaerobic conditioning was conducted for the partially saturated sediment column by applying six cycles of vacuum and then nitrogen gas over the course of an hour, after which, the columns were flushed with 400 pore volumes of helium to remove any trapped air in sediment dead end pores. Cr(VI) loading consisted of injecting Hanford groundwater (anoxic, degassed with continuous helium bubbling) containing 300 µg/L of Cr(VI) into the sediment column for 6 to 10 pore volumes with the goal of obtaining a uniform Cr(VI) concentration in the pore water throughout the soil column. A high-performance liquid chromatography (HPLC) pump (Hitachi L6200) was used to maintain a constant injection rate for the loading process. During Cr(VI) loading, effluent Cr(VI) concentrations were within 5% of the influent concentration within two pore volumes. After the Cr(VI) loading, the column inlet and outlets were sealed with valves (HIP 1.16” low volume). The Cr(VI) reduction experiment consisted of manual injection of 1.5 mL (0.06 pore volumes) of anoxic, Cr(VI)-free Hanford groundwater at the column inlet and collection of effluent samples at the column outlet. Effluent samples were analyzed for Cr(VI) concentration. This Cr(VI)-reduction experimental procedure enabled measurement of the pore-water Cr(VI) concentration over time at the high sediment-to-water ratio where the soil columns were considered as a batch (non-flowing) configuration for the test. The first 0.5 mL of effluent was not used (because there was an estimated 0.25 mL of liquid in the effluent frit). The sampling procedure was applied 7 to 14 times to track changes in Cr(VI) concentration for time periods of up to 1200 hours.

Table 2. Cr(VI) reduction experimental matrix.

Experiment	Description	Sediments
1	Batch Cr(VI) reduction under anoxic conditions in soil columns.	14, 15, 16, 17, 18, 19
2	Batch Cr(VI) reduction under anoxic conditions in soil columns with sediments pre-treated with biocide.	14
3	Batch Cr(VI) reduction under anoxic conditions in soil columns with added microbial substrate (lactate).	17
4	Batch Cr(VI) reduction under anoxic conditions in soil columns with sediments treated with 1% hydrogen peroxide.	14
5	Batch Cr(VI) reduction under anoxic conditions in soil columns. Sediments were then exposed to dissolved oxygen and the anoxic experiment repeated.	17
6	Batch Cr(VI) reduction under oxic conditions in soil columns.	14, 17
7	Batch Cr(VI) reduction under anoxic conditions in soil columns with field-contaminated sediments.	5, 10
8	Cr(VI) reduction under anoxic conditions at low sediment-to-water ratio to evaluated reduction capacity.	14

Several variations of the above procedures and control experiments were conducted to help evaluate Cr(VI) reduction in these sediments. In some experiments, the Cr(VI) loading and Cr(VI) reduction components were repeated after concentrations in the initial Cr(VI) reduction experiments dropped below 5 µg/L (the analysis detection limit). Several experiments were conducted to investigate the influence of biotic reactions on Cr(VI) reduction. Negative microbial control experiments consisted of the addition of gluteraldehyde or potassium cyanide as biocides. A solution of 2% gluteraldehyde in Hanford groundwater with no Cr(VI) was mixed with sediment (2 mL/g-sediment) for 5 days. This sediment was then used in a batch Cr(VI)-reduction experiment, as described above, except that 2% gluteraldehyde was added to the injected solutions. In a separate experiment, 5 mg/L potassium cyanide was added to the injected solutions for the Cr(VI)-reduction experiments. As a positive control for biotic activity, 5 mg/L lactate was added to the injected solutions for the Cr(VI)-reduction experiments. Additional experiments were conducted using oxic Hanford groundwater (8.2 mg/L dissolved oxygen) for the Cr(VI) loading and Cr(VI) reduction components of the experiment. As another evaluation of the effect of dissolved oxygen on the Cr(VI) reduction capacity of the sediments, in some experiments, 20 pore volumes of oxic Hanford groundwater (8.2 mg/L dissolved oxygen) were flowed through the column after concentrations in the initial Cr(VI) reduction experiments dropped below 5 µg/L (the analysis detection limit). The Cr(VI)-reduction experiment as described above, was then repeated for these columns.

In addition to testing sediments with no initial Cr(VI) (non-detect concentrations [CHPRC 2015]), Cr(VI) reduction experiments were conducted with field-contaminated sediments. These tests were conducted by packing the Cr(VI)-contaminated sediments into the soil column and then conducting the Cr(V) reduction component of the experiment without the anaerobic preconditioning and without the Cr(VI) loading components.

A few chromate reduction experiments were conducted in a septa-top glass vial at a low sediment/water ratio (0.52 g-sediment/mL-water) under anoxic conditions with Hanford groundwater (anoxic, degassed with continuous helium bubbling) containing 300 µg/L of Cr(VI) concentration to evaluate the reduction capacity of the sediment. This experimental configuration had a much higher ratio of Cr(VI) mass to sediment mass so that a total capacity of Cr(VI) reduction could be evaluated. In one sediment control experiment, sediment was oxidized with 1% hydrogen peroxide for 5 days prior to conducting the Cr(VI)-reduction experiment. The hydrogen peroxide experiment was conducted to evaluate the impact of a harsh oxidant expected to fully oxidize the sediments and act as a biocide. Several additional control experiments were conducted to evaluate potential experimental artifacts. A 330 µg/L Cr(VI) standard was measured at multiple times over a period of 250 hours in 1) a vial containing oxic deionized water, 2) a vial containing oxic Hanford groundwater, and 3) anoxic Hanford groundwater in the stainless-steel column with no sediment.

After concentrations in the Cr(VI) reduction experiments dropped below 5 µg/L (the analysis detection limit) for some of the sediments, the remobilization (and potential oxidation) of chromium was investigated by injection of 20 pore volumes of oxic Hanford groundwater into the sediment column. Oxic Hanford groundwater (8.2 mg/L dissolved oxygen) was injected into the column at a constant rate using an HPLC pump and ~40 effluent samples were collected. The frequency of effluent sampling was varied to collect more samples at selected times. Because some Cr(VI) may be adsorbed to sediment, 12 effluent samples were collected during the first three pore volumes. The remaining effluent samples were collected at less frequent intervals. Effluent samples were analyzed for Cr(VI) concentration.

2.2 Investigation of Cr(VI) Solid Phases

The characteristics and behavior of solid-phase Cr(VI) phases were investigated in leaching studies, using solid-phase characterization techniques, and in experiments examining co-precipitation and dissolution of Cr(VI) with calcium carbonate.

2.2.1 Cr(VI) Leaching Experiments

Sediment from the liners selected for soil column leaching tests (Table 1, sediments 1−12) were emptied and sieved to remove particles greater than 4 mm. The total liner sediment weight and all larger particles were retained for use in data analysis calculations. The field moisture content on the <4 mm fraction was also determined by wet and dry weights using a separate sediment sample.

Sieved material was packed into 1 in. diameter by 6 in. long soil columns. High-performance liquid chromatography pumps were used to inject simulated groundwater upward (soil column mounted vertically) through the column with a residence time of about 4 hours. This residence time corresponds to a linear velocity of water through the soil column of about 3 ft/d. The groundwater velocity in the aquifer where the samples were collected varies seasonally, so a single column flow rate is not directly representative of field conditions. In addition, flow through the aquifer is heterogeneous due to the heterogeneous hydraulic conductivity in the aquifer. Thus, experiments used a reasonable flow rate and stop-flow events to obtain leaching data suitable to evaluate rapid (equilibrium) and kinetically controlled processes (i.e., due to physical limitations such as diffusion from stagnant pore space or chemical limitations such as a relatively slow surface reaction or dissolution of less reactive coatings exposing reactive surfaces). Flow continued for 400 to 900 hours. Effluent was collected using a fraction collector and selected time interval samples analyzed for Cr(VI) and total chromium (EPA Method 7196), bromide, and pH. A bromide tracer was used to evaluate the flow conditions in the column based on the breakthrough pattern of bromide. At selected times, flow was stopped for either 16 to 280 hours to allow any surface phase Cr(VI) to equilibrate with the pore water as a means to evaluate the Cr(VI) release rate from sediment. The difference in Cr(VI) concentrations before and after the stop-flow event was used to calculate a rate of Cr(VI) release from the sediment.

Water extractions at a ratio of 1.0 g of sediment to 1.0 mL of deionized water were conducted at several time intervals to extract chromium from pore water and sediment to compare these results with leaching results. Because leaching is essentially water extraction over 100s of hours and some of the leached chromium is the result of slow release from sediment, batch water extractions were conducted over 1 hour, 24 hours, and 7 days to evaluate the kinetics of chromium slow release from sediment. The alkaline digestion of the sediment for Cr(VI) (EPA Method 3060A) was also used as a batch extraction of the total chromium in the sediment. This method is specifically designed to not reduce native Cr(VI) to Cr(III). It should solubilize water-insoluble and water-soluble Cr(VI) compounds. However, EPA Method 3060A states "This method uses an alkaline digestion to solubilize both water-insoluble (with the exception of partial solubility of barium chromate in some soil matrices, see Reference 10.9) and water-soluble Cr(VI) compounds in solid waste samples." The chromate-substituted Ca-carbonate identified in this study may not be fully dissolved in this alkaline extraction. The alkaline digestion uses 0.28 M Na_2CO_3 and 0.5 M NaOH at 95^oC for 60 minutes to dissolve the Cr(VI) and stabilize it against reduction to Cr(III).

2.2.2 Surface-Phase Characterization

Surface-phase characterization was conducted by electron microprobe (EMP) and elemental analysis for 1) vadose zone sediments to identify/characterize high-concentration chromium precipitates and 2) aquifer sediments to identify chromium phases before and after leaching. Chromium precipitates were characterized by EMP with a JEOL JXA-8230 electron probe microanalyzer and for elemental analysis with an energy-dispersive x-ray spectroscopy detector. Vadose zone sample preparation consisted of attaching sediment particles to a dielectric cap on a microprobe mount and carbon coating. The EMP provided images of crystalline particles at different magnifications (40x to 60,000x) and elemental analysis at the 2 µm scale to identify chromate-containing precipitates. Chromate precipitates on pre- and post-leach aquifer sediments were present at lower concentrations than for vadose zone sediments and were characterized by collecting elemental (Cr, Fe, S, Ba, Si, Ca, Al, C, O) maps (750 by 750 points, 1 µm resolution) of sediment grains in an epoxy thin section. Elemental analysis was quantitative by comparison of element intensities to standards using the same elemental detector. The three aquifer sediments with the highest chromium concentration were used in EMP analysis (Table 1, sediments 4, 5, and 10). The objective of the analysis was to evaluate chromium associations with 1) calcium (i.e., Cr(VI) co-precipitation with calcium carbonate), 2) iron (i.e., $CrIII(OH)_3$ or $(Cr, Fe)(OH)_3$ precipitates), or 3) barium (i.e., $BaCrO_4$).

2.2.3 Uptake and Release of Cr(VI) by Calcite or Other Carbonate Minerals

Batch experiments with different initial Cr(VI) aqueous concentrations were conducted to study Cr(VI) co-precipitation with calcium carbonate. This study followed the methods of Hua et al. (2007) for their similar study of Cr(VI) co-precipitation at high initial Cr(VI) concentrations (~190 to 9700 mg/L). Three sets of batch experiments were conducted at room temperature and open to the atmosphere.

Carbonate mineral precipitation at different initial Cr(VI) aqueous concentrations. Treatments containing 30 µg/L, 1 mg/L, 5 mg/L, 30 mg/L, or 100 mg/L of Cr(VI) were prepared in 1 M solutions of $CaCl_2$ (125 mL). This solution was mixed with 125 mL of a 1 M sodium carbonate solution in a 250 mL Nalgene bottle. The supernatant was subsequently sampled after 4, 8, 24, and 72 hours. Cr(VI) concentration was measured in these solutions using a Perkin Elmer 8300 DV inductively coupled plasma-optical emission spectrometer (ICP-OES). The resulting solid phase was analyzed by X-ray diffraction (XRD) and scanning electron microscopy to confirm the presence of different calcium carbonate minerals, such as vaterite and calcite.

2.3 Aqueous-Phase Analyses

Cr(VI) was measured by reaction with 1,5- diphenylcarbazide (EPA Method 7196A, Hach Method 8023). This method is highly selective for Cr(VI) and has few interferences, including when used on alkaline digestion samples. Additional acid was needed for the alkaline digestion samples to achieve a final pH of 2.0 ± 0.5 for the Cr(VI)-diphenylcarbazide reaction (Pflaum and Howick 1956). For example, in laboratory experiments with groundwater samples, 20 µL of nitric acid added to 2 mL of water was sufficient to reach the target pH, whereas for analysis of the alkaline digestion samples, 260 µL of nitric acid were needed. A daily 7-point calibration curve was used over a range of 0 to 500 µg/L Cr(VI). Duplicate samples were measured every 5 samples and a standard was measured every 10 samples. Total chromium was measured on some samples by inductively coupled plasma optical emission spectroscopy (ICP-OES).

Bromide was measured with an ion-specific electrode (Accumet 13-620-525), with 9-point calibration before each experiment and a calibration check after measurements. The pH was measured with a microelectrode (Accumet 13-602-292) with 3-point calibration before measurements and a calibration check after measurements.

3.0 Results

A series of experiments were conducted to evaluate natural attenuation mechanisms in Hanford 100 Area sediments. These experiments investigated chemical reduction of Cr(VI) and the factors related to the rate of reduction under natural attenuation conditions (Section 3.1). Attenuation through formation of solid-phase compounds was also investigated (Section 3.2). Sorption is also a component of natural attenuation, but was not evaluated in this study.

3.1 Hexavalent Chromium Attenuation Data

A series of laboratory-scale measurements provided evidence of Cr(VI) reduction in the Hanford 100 Area sediments. Loss of Cr(VI) was observed in stop-flow soil column experiments loaded with anoxic groundwater containing 300 µg/L Cr(VI) for five different sediment samples, four from the Hanford 100 Area and one from the Hanford 200 East Area (Figure 1). The rate of chromate reduction in these different sediments varied. This variation is likely due to a combination of influences from the sediments containing differing amounts of facies that can reduce Cr(VI) and the different reduction rates for different types of reducing facies. Cr(VI) was reloaded into one of these experiments and the Cr(VI) loss over time was nearly identical to results with the initial loading (Figure 2). For this sample, the capacity for Cr(VI) reduction had not been met with the two loadings of 300 µg/L Cr(VI) into the soil column. A batch experiment with one of the sediments with a higher water-to-sediment ratio (40 mL-water/20 g-sediment) was conducted to evaluate the total Cr(VI) reduction capacity (Figure 3). The calculated reductive capacity of this 100-D sediment is 0.062 µmol electrons/g. For a field-relevant water-to-sediment ratio (e.g., a packing density similar to the soil column packing), this observed capacity is equivalent to reduction of about 16 pore volumes of Cr(VI) at a concentration of 300 µg/L.

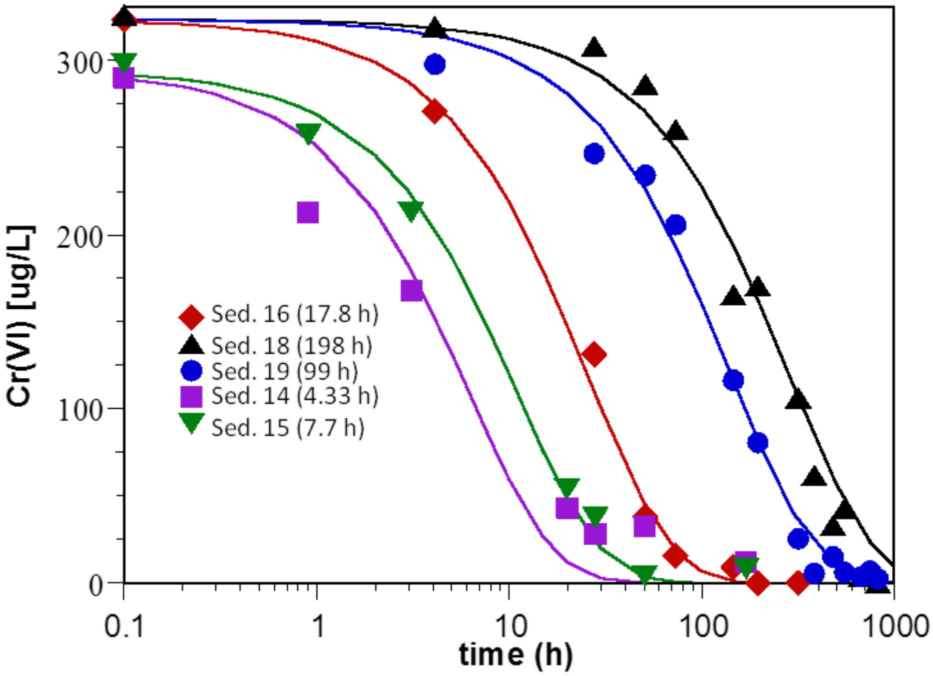

Figure 1. Decrease in Cr(VI) concentrations observed under anoxic conditions. Numbers in parentheses are the half-life for a first-order equation fit to the data.

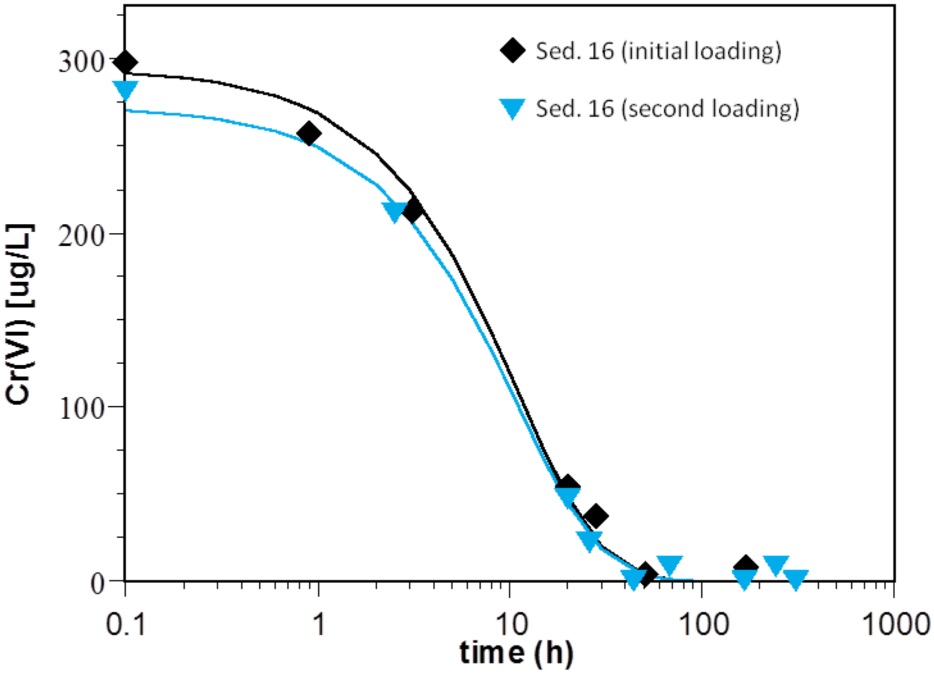

Figure 2. Decrease in Cr(VI) concentrations observed under anoxic conditions for the initial loading of Cr(VI) in the experiment and for the same column with Cr(VI) loaded a second time. Lines are a first-order equation fit to the data where both sets of data have a computed half-life of 7.7 hours.

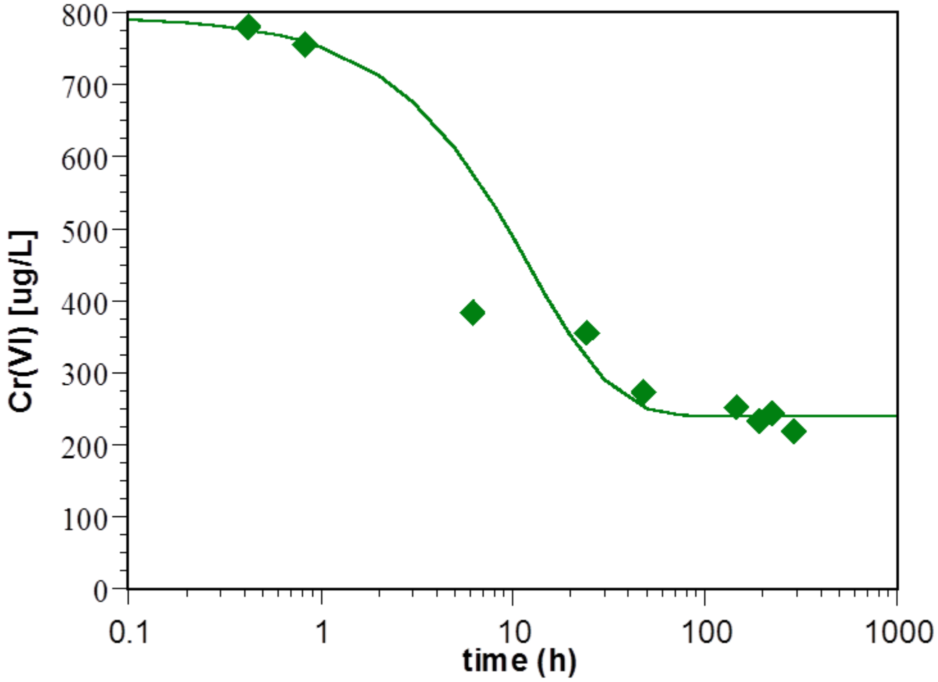

Figure 3. Decrease in Cr(VI) concentrations observed under anoxic conditions in an experiment with a low sediment-to-water ratio with sediment 14 (Table 1). The lines are a fit to the data with a computed half-life of 8.7 hours assuming a starting concentration of 800 µg/L and a final concentration of 250 µg/L.

Presence of dissolved oxygen is important to consider in evaluating the potential for Cr(VI) as an attenuation mechanism in the Hanford 100 Area aquifer. The Cr(VI) reduction in Figure 1 through Figure 3 was observed under conditions where anoxic groundwater containing Cr(VI) was introduced to the soil columns. The test was repeated for two sediments using oxic groundwater containing Cr(VI) (Figure 4 and Figure 5). In both cases, the rate of Cr(VI) reduction was slower, but still occurred. For one case the rate was an order of magnitude slower (Figure 4). In the other sediment, the rate was only about 50% slower (Figure 5). As another test, the same soil that was used for the anoxic results shown in Figure 4 was exposed to oxic groundwater for 20 pore volumes after completion of the initial test. This column was then exposed again to anoxic groundwater containing Cr(VI), and Cr(VI) reduction was observed at a rate that was about a factor of 4 slower than the rate for the initial test (Figure 6). While dissolved oxygen did not completely suppress Cr(VI) reduction in these tests, treatment of the sediments with 1% hydrogen peroxide, expected to fully oxidize the sediments and kill microorganisms, did stop Cr(VI) reduction (Figure 4). These results suggest that the sediments, as analyzed, did contain measureable reductive capacity and that the reductive capacity for Cr(VI) can be active in the presence of dissolved oxygen.

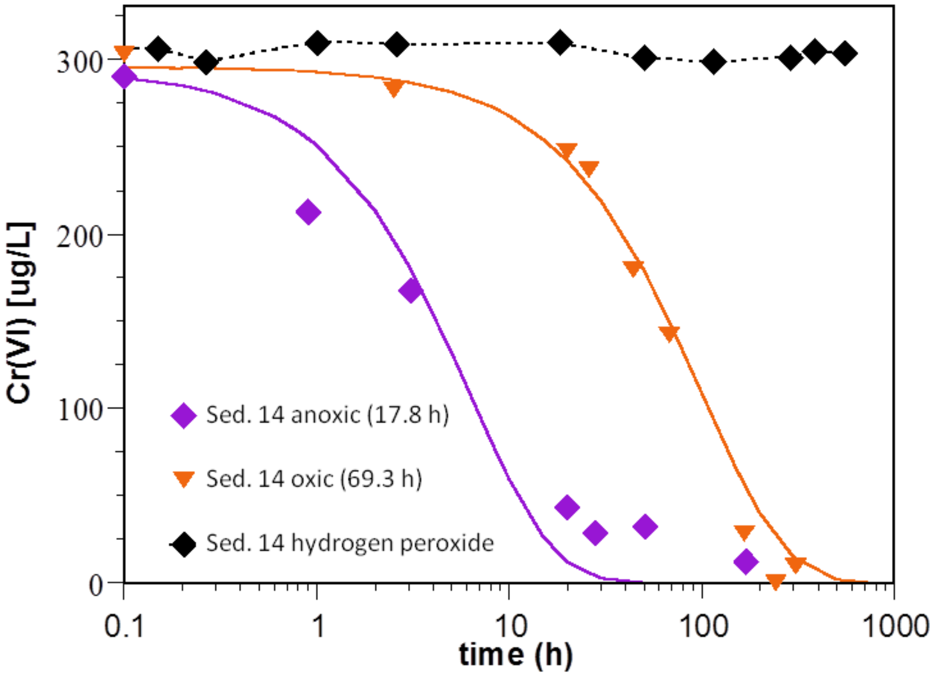

Figure 4. Decrease in Cr(VI) concentrations observed under anoxic and oxic conditions. Numbers in parenthesis are the half-life for a first-order equation fit to the data. Data are also shown for an experiment where the sediment was pre-treated with 1% hydrogen peroxide as a harsh oxidant and as a biocide.

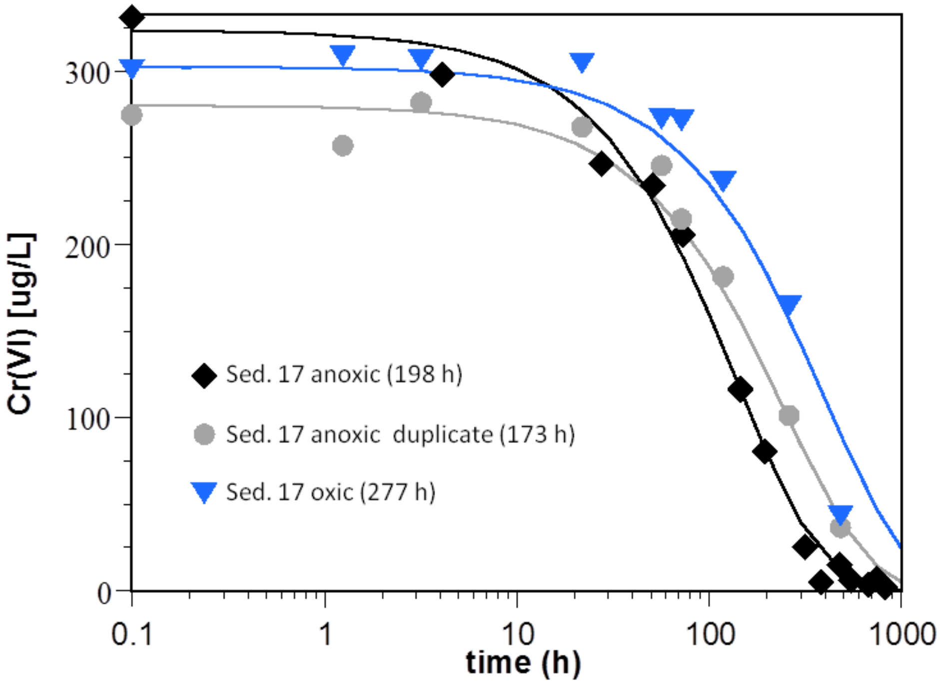

Figure 5. Decrease in Cr(VI) concentrations observed under anoxic (in duplicate) and oxic conditions. Numbers in parenthesis are the half-life for a first-order equation fit to the data.

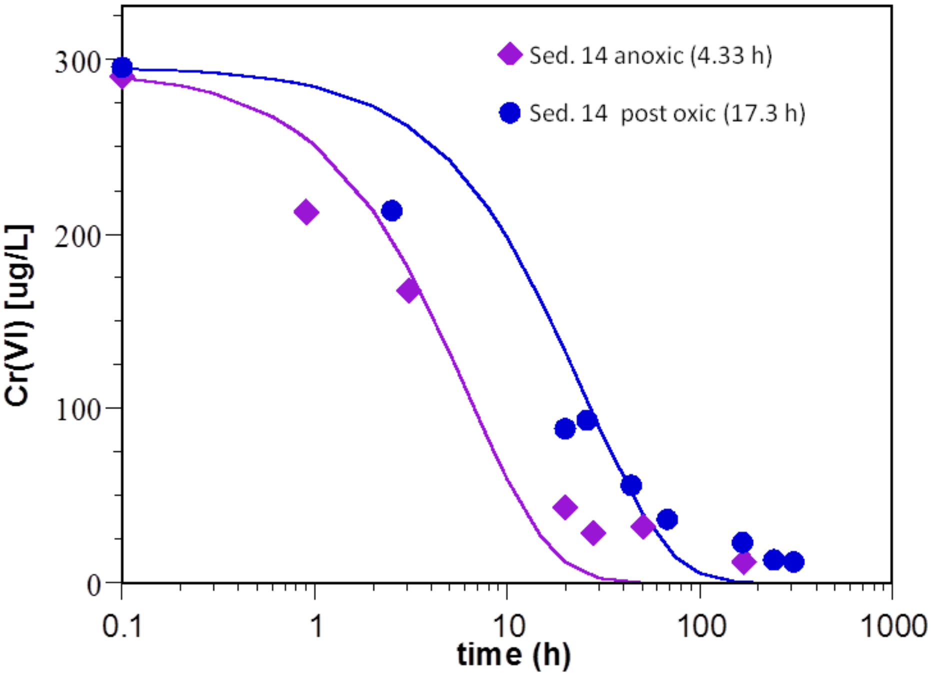

Figure 6. Decrease in Cr(VI) concentrations observed under anoxic conditions and for an experiment where this same column was exposed to 20 pore volumes of oxic Hanford groundwater and then the anoxic experiment repeated (post oxic). Numbers in parenthesis are the half-life for a first-order equation fit to the data.

The above test results were for sediments containing negligible initial Cr(VI) contamination and Cr(VI) was introduced into the column for the test. Additional tests were conducted for two sediments that contained actual field-derived Cr(VI) contamination. Soil column leaching tests with oxic groundwater showed release of Cr(VI) over time from these sediments (Figure 7). The release rate was slower than would be expected if only dissolved and sorbed phase Cr(VI) were present as described in Section 3.2. Aliquots of these same sediments were used in soil column tests with anoxic groundwater (same test protocol as for the other reduction soil column tests) and showed Cr(VI) reduction over time (Figure 8). Thus, under the slower stop-flow conditions and with anoxic groundwater, Cr(VI) reduction was observed in these contaminated sediments.

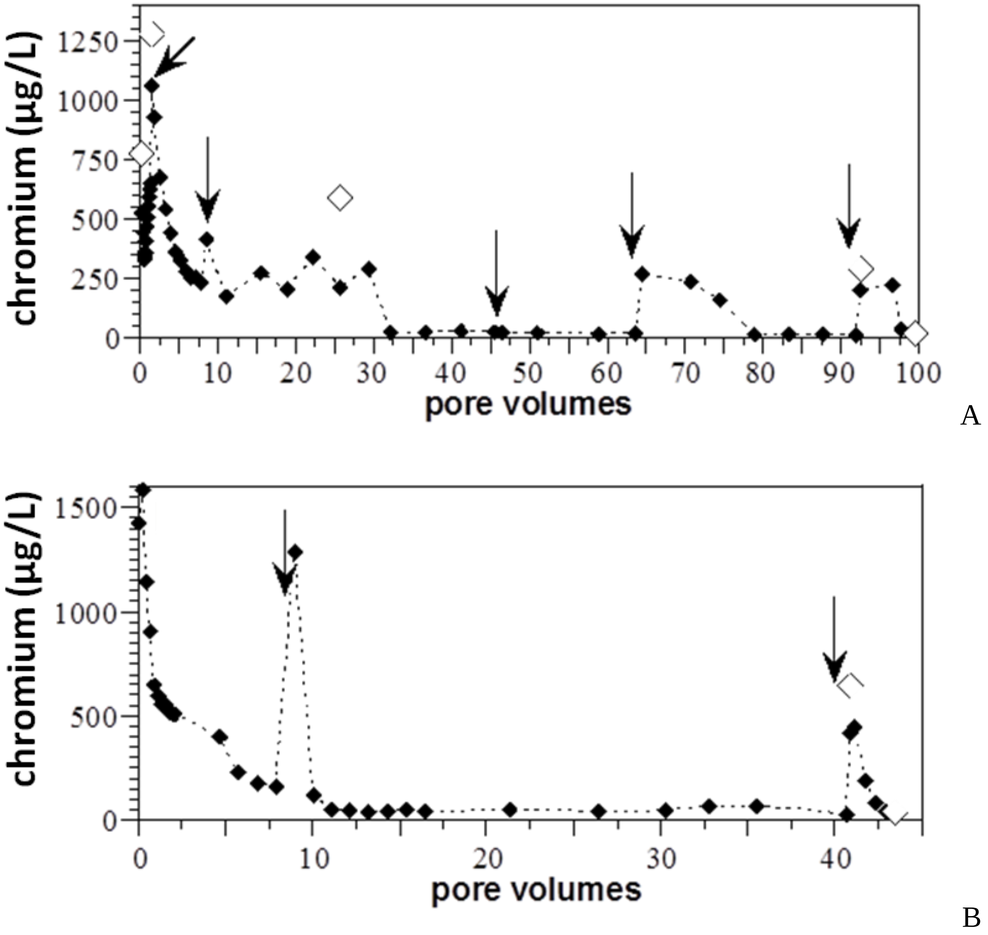

Figure 7. Cr(VI) (solid diamonds) and total chromium (open, large diamonds) concentrations in the effluent of a soil column leaching tests for field-contaminated A) sediment 5 and B) sediment 10. Additional descriptions of leaching experiments are in Section 3.2. Arrows denote stop flow intervals.

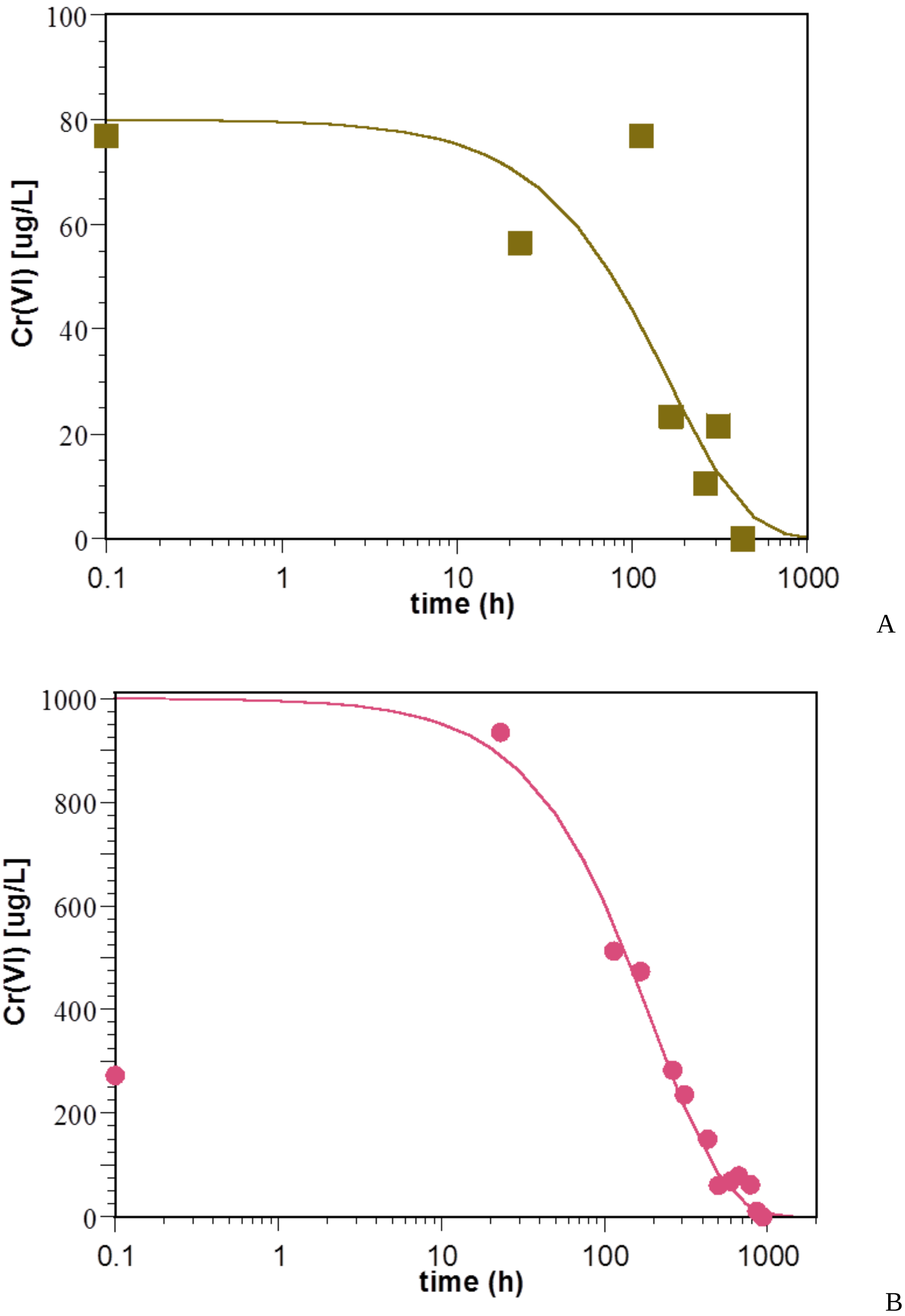

Figure 8. Decrease in Cr(VI) concentrations observed under anoxic conditions in an experiment with field-contaminated A) sediment 5 (half-life of 116 h for a first-order equation fit to the data) and B) sediment 10 (half-life of 139 h for a first-order equation fit to the data) that were also used in soil column leaching tests (Figure 7).

In addition to conducting the control experiment with 1% hydrogen peroxide (described above), additional controls were conducted to help verify that Cr(VI) losses were not from other mechanisms. The following controls showed no observed Cr(VI) loss over a period of 1000 hours: 1) a Cr(VI) standard in oxic, deionized water (Cr(VI) concentrations were ± 1.56% over the test duration), 2) a Cr(VI) standard in groundwater to show that carbonate-laden water does not cause Cr(VI) precipitation (Cr(VI) concentrations were ±2.26% over the test duration), and 3) Cr(VI) in anoxic groundwater in the steel experimental column to show that Cr(VI) is not reduced by the steel column used for the tests (Cr(VI) concentrations were ±2.44% over the test duration).

A final set of tests was conducted to evaluate the relative contribution of biotic and abiotic Cr(VI) reduction processes. One test compared observed Cr(VI) reduction in anoxic groundwater for tests with no sediment alteration, with addition of cyanide as a biocide, and with addition of gluteraldehyde as a biocide. Sediments were contacted with the biocides for 5 days before conducting the Cr(VI) reduction tests. Figure 9 shows that use of the biocides reduced the Cr(VI) reduction rate by a factor of about 5. It is also possible that the biocide affected some of the abiotic reduction capacity of the sediments as part of this observed decrease in the reduction rate. A test with the addition of 5 mg/L lactate as a substrate for biotic activity was conducted as a positive control for biotic reduction (though at very low concentration not intended to represent full biostimulation as would be applied for bioremediation). Figure 10 shows that addition of the substrate induced a minor increase in the Cr(VI) rate. Abiotic reductive capacity is most likely related to ferrous iron compounds in the sediments. Sediment characterization for sediments 5, 8, 10, 15, 16, and 18 showed that ferrous iron phases accounted for about one-third of the iron in the sediments.

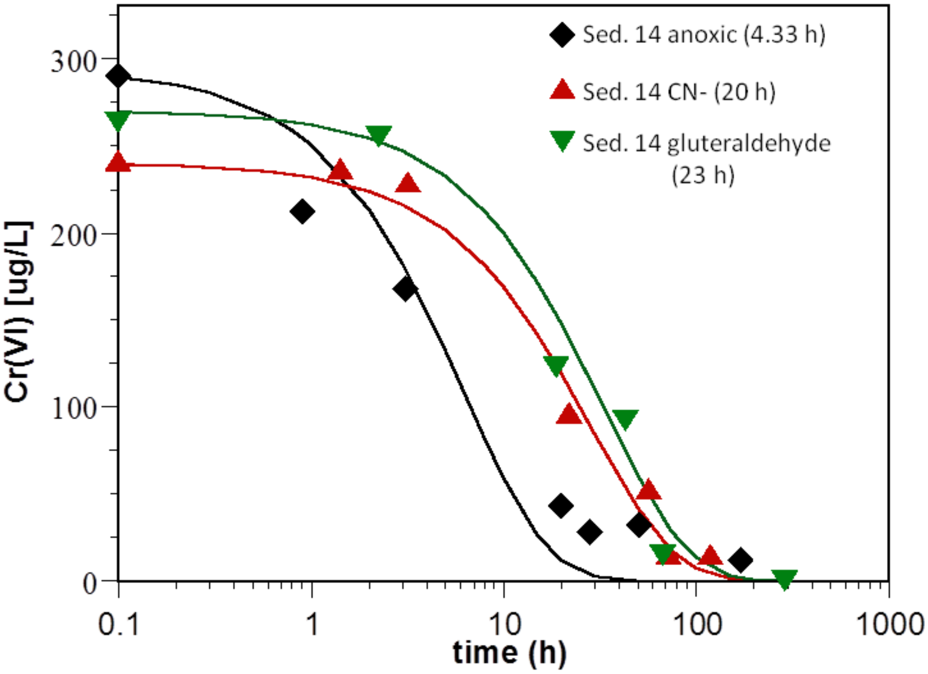

Figure 9. Decrease in Cr(VI) concentrations observed under anoxic conditions with a sediment pre-treated with either 5 mg/L potassium cyanide or 2% gluteraldehyde as biocides. The same sediment without biocide treatment is also shown for comparison. Numbers in parentheses are the half-life for a first-order equation fit to the data.

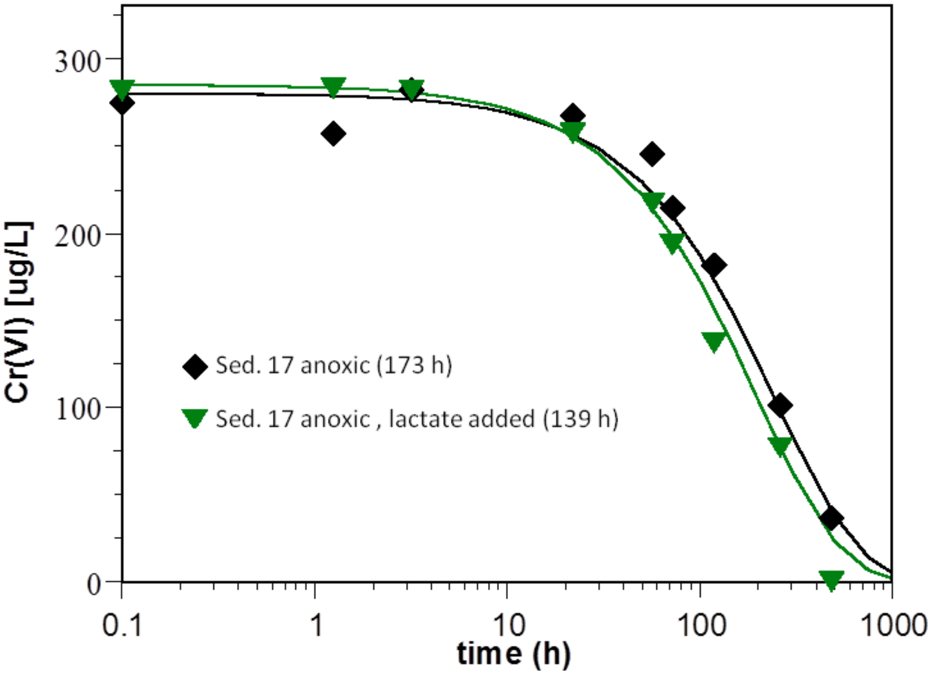

Figure 10. Decrease in Cr(VI) concentrations observed under anoxic conditions with a sediment amended with 5 mg/L sodium lactate. The same sediment without amendment is also shown for comparison. Numbers in parentheses are the half-life for a first-order equation fit to the data.

3.2 Hexavalent Chromium Solid-Phase Associations Related to Source Zones and Plume Attenuation

Leaching experiment data and solid-phase characterization data were collected to describe Cr(VI) associated with solid phases that may be important in quantifying Cr(VI) sources and as part of attenuation mechanisms. In addition, co-precipitation of Cr(VI) with calcium carbonate was investigated in relation to its potential to act as an attenuation mechanism downgradient of source zones.

Aquifer and vadose zone samples collected at the 100-D-100 source remediation site contained elevated Cr(VI) concentrations that show characteristics of slow release in soil column leaching tests (Figure 11). In these experiments, leaching of mobile Cr(VI) species would be expected to occur within a few pore volumes of sediment flushing, because bromide tracer results showed a sharp breakthrough of injected water (i.e., little dispersion) at near one pore volume (CHPRC 2015). However, across a wide range of Cr(VI) contaminant levels, Figure 11 shows extended duration release of Cr(VI) from the sediment and evidence of slow release based on concentration increases during stop-flow events (i.e., Figure 11a through d). These same conclusions are evident in **Figure 12**, which shows the cumulative Cr(VI) mass leached from the column for all of the sediments tested. For most sediments, there was an initial quick release of mobile Cr(VI) (steep initial rise in the cumulative effluent mass) followed by a slower increase in the cumulative effluent Cr(VI) mass over tens of pore volumes.

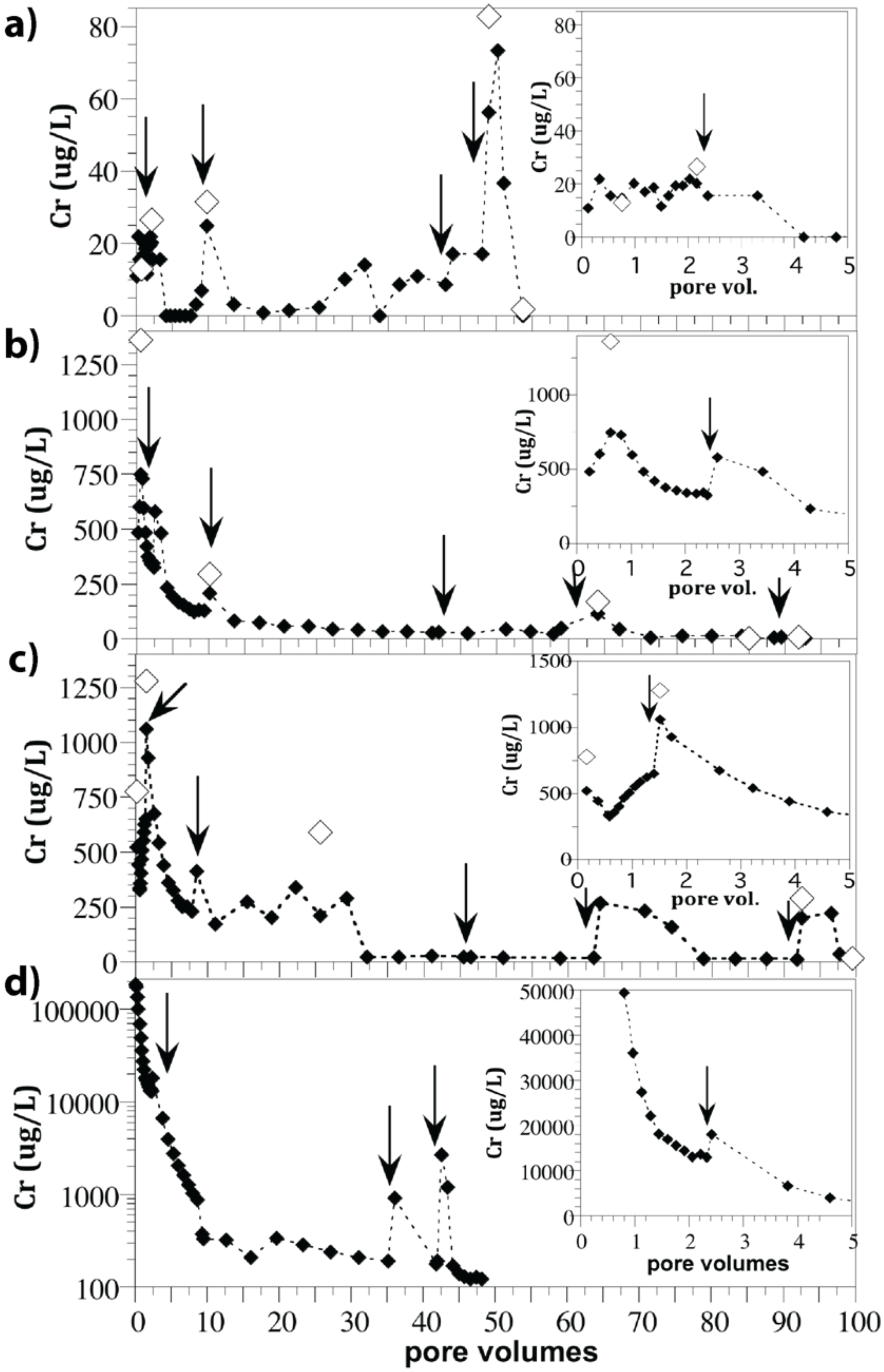

Figure 11. Leaching of Cr from subsurface sediments from: a) sediment 1, b) sediment 4, c) sediment 5, and d) sediment 11, as shown by Cr(VI) (black diamonds) and total Cr (open diamonds). Arrows denote a stop-flow interval. Inset graphs show the first five pore volumes.

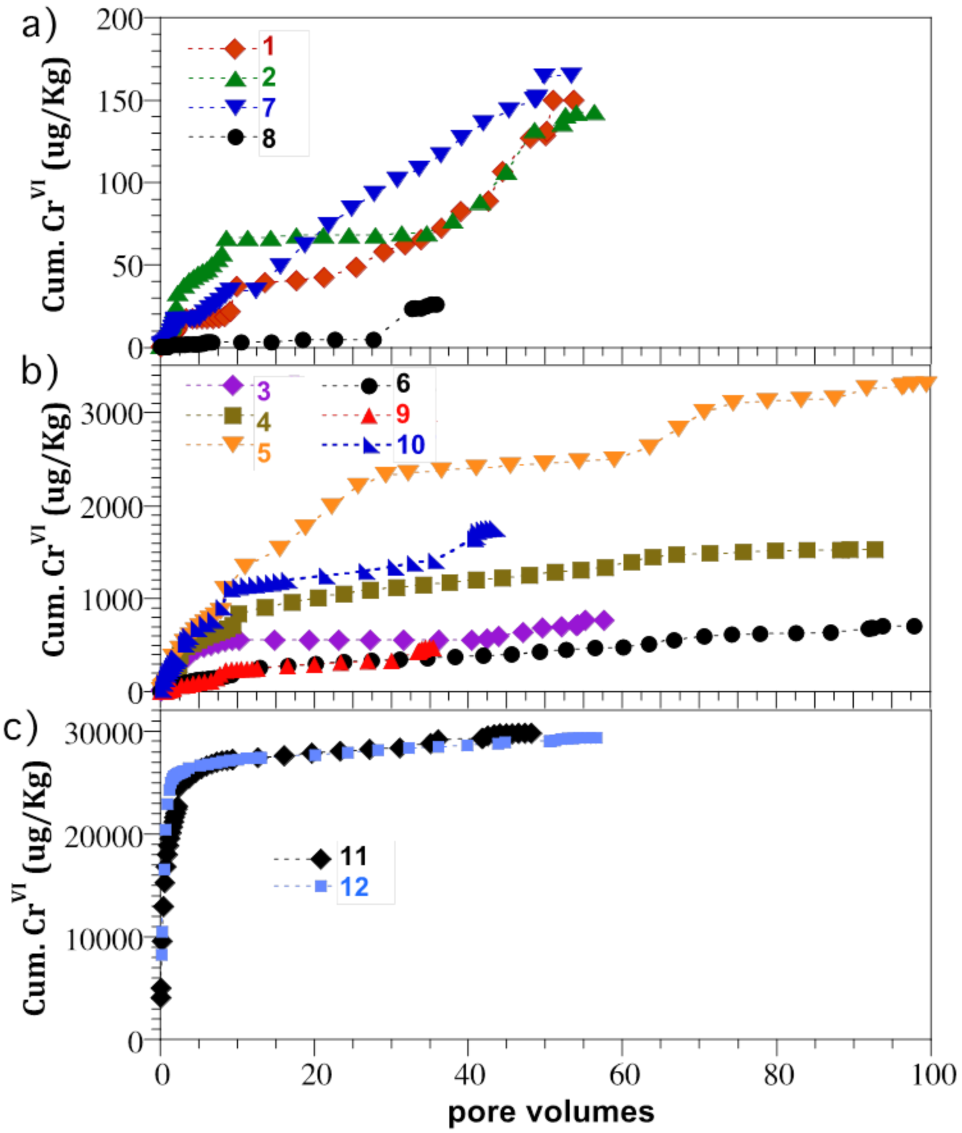

Figure 12. Cumulative Cr(VI) mass during leaching experiments for a) low Cr(VI) aquifer sediments, b) high Cr(VI) aquifer sediments, and c) high Cr(VI) vadose zone sediments.

Analysis of sediment samples before and after leaching with tens of pore volumes of groundwater provides additional evidence that there is Cr(VI) in the sediment associated with solid phases.

Table 3 shows that even after leaching, there is Cr(VI) in the sediment samples that can be extracted with groundwater and a greater amount of Cr(VI) that can only be extracted using an alkaline solution (e.g., associated with a solid phase). In many of the aquifer samples, only a small portion of the total mass of Cr(VI) was leached by groundwater over tens of pore volumes. In contrast, in vadose zone samples, which contained relatively high concentrations of Cr(VI), most of the Cr(VI) mass was leached in the tests. Cr(VI) precipitates in vadose zone samples may have been recently deposited as part of evaporative concentration rather than the longer-term processes associated with persistent Cr(VI) solid phases in the aquifer (CHPRC 2015).

Table 3. Total Cr and Cr(VI) mass (µg/kg) of pre- and post-leached sediments.

Sediment Number	Pre-Test Cr(VI) Water Extraction	Pre-Test Cr(VI) Alkaline Extraction	Pre-Test Total Cr Alkaline Extraction	Cr(VI) Leached	Post-Test Cr(VI) Water Extraction	Post-Test Cr(VI) Alkaline Extraction	Post-Test Total Cr Alkaline Extraction	Fraction Leached(a)	Mass Balance	Bromide Tracer Column Retardation
1	3.14			149.8	102.5	2498	1690			1.076
2	113.1	2628	2700	142.9	3.142	1590	1890	5	66	1.014
3	439.8	3864	5160	766.1	62.83	1857	1660	20	68	0.867
4	455.5	4201	5360	1531	3.142	2925	2390	36	106	1.078
5	252.9	3864	5140	3297	47.12	1964	1870	85	136	0.956
6	232.5	2684	2860	705.1	3.142	1270	1410	26	74	1.005
7	147.7	2178	2540	164.9	21.99	2605	1860	8	127	1.122
8	91.4	3077	1520	25.8	ND	ND	ND	1	ND	0.919
9	53.4	1673	2410	469.4	ND	ND	ND	28	ND	1.083
10	504.6	4650	4160	1757	ND	ND	ND	38	ND	0.922
11	22,120	34,520	49,900	28,817	ND	ND	ND	83	ND	ND
12	25,240	28,950	45,000	28,787	ND	ND	ND	99	ND	ND

ND = no data.

(a) Computed as Cr(VI) leached (as µg/kg) divided by pre-test Cr(VI) alkaline extraction.

Solid-phase investigations were conducted to improve understanding of the materials causing the observed slow Cr(VI) leaching in the soil columns and evaluate the potential solid phases that remained after leaching. Because vadose zone samples were available with visual evidence of Cr(VI) contamination based on yellow staining, samples were obtained and the yellow stained material was analyzed by EMP. The yellow material was identified as Cr(VI) co-precipitated with calcium carbonate (i.e., a $CaCrO_4$ precipitate) (Figure 13). Thus, co-precipitated Cr(VI) with calcium carbonate is one type of solid-phase Cr(VI) material that is present at the 100-D-100 source area and may contribute to the observed leaching behavior. Aquifer samples could not be examined in the same way because there was no visual indication of Cr(VI) contamination to focus the analysis. However, a scanning process was applied that enabled information from these lower-concentration samples to be obtained. The scans revealed locations with apparent associations of elements that can be interpreted as indicating different types of chromium materials. Scans were conducted on both pre- (Figure 14) and post-leaching (Figure 15) sediments. Chromium was observed to be associated with calcium, barium, and iron. Iron had a low association with sulfur, so it is not likely a ferrous sulfide phase, rather, it is more likely an iron oxide. The chromium association with calcium is interpreted to be Cr(VI) co-precipitated with calcium carbonate, a material similar to that analyzed for vadose zone sediments (Figure 13). The chromium associated with barium is interpreted to be a barium chromate mineral, which would have a low solubility. The chromium associated with iron could be either Cr(VI) or Cr(III) sorbed to, or incorporated into, an iron oxide deposit (the analysis technique cannot differentiate between Cr(VI) and Cr(III)). All of these materials were observed in both pre-and post-leaching samples and, therefore, represent a Cr(VI) solid phase that has some resistance to leaching. Thus, it is unlikely that the observed chromium associated with iron in the post-leaching experiments was sorbed. It is possible that some of the observed chromium was Cr(III) because tests with some of these aquifer sediments showed Cr(VI) reduction potential (Section 3.1).

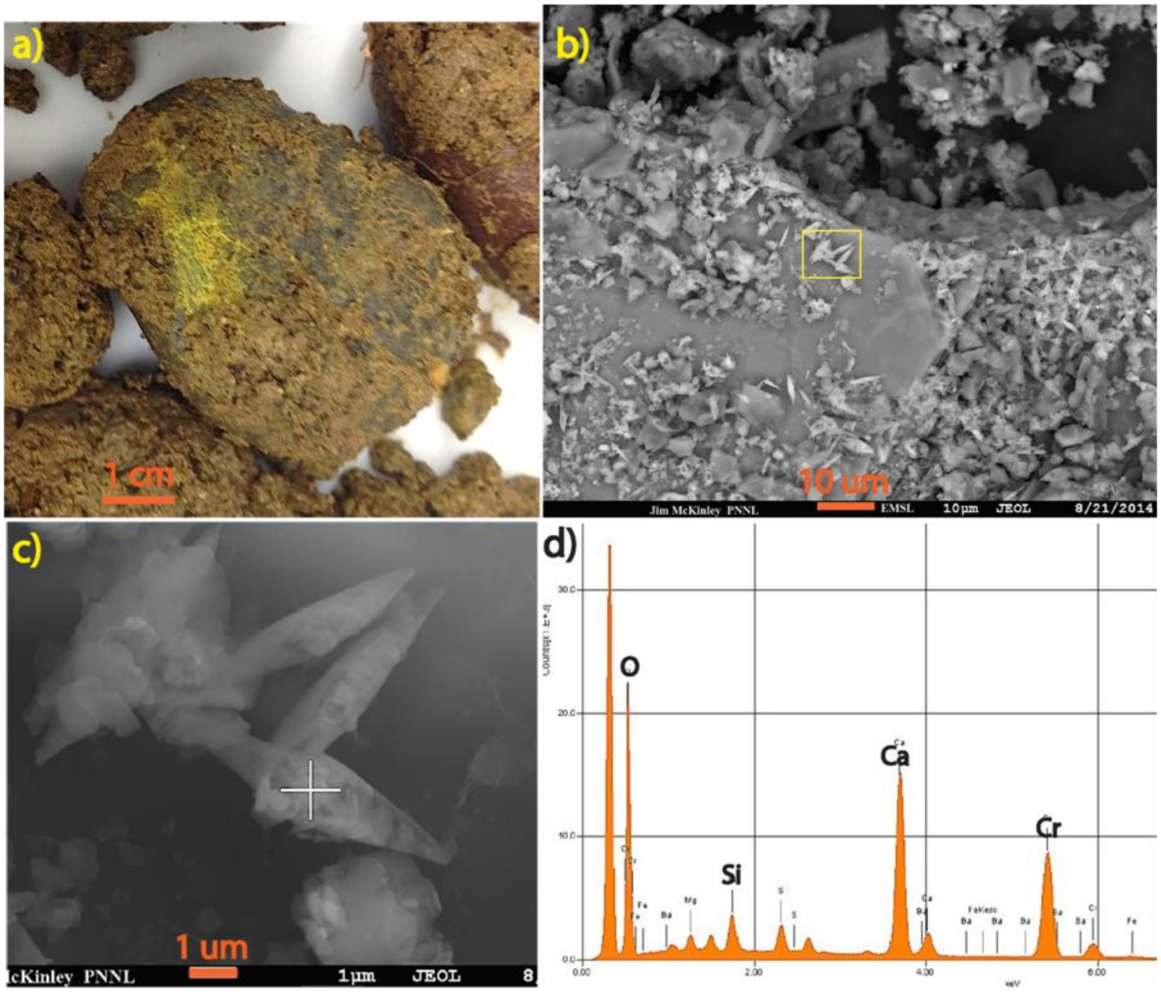

Figure 13. Images of sediment 13: a) photograph of gravel (4 cm length) with fine yellow precipitate, b) electron microprobe electron backscatter image of fine bladed precipitates, c) electron microprobe electron backscatter image of bladed precipitates, and d) elemental analysis of chromate-substituted calcite.

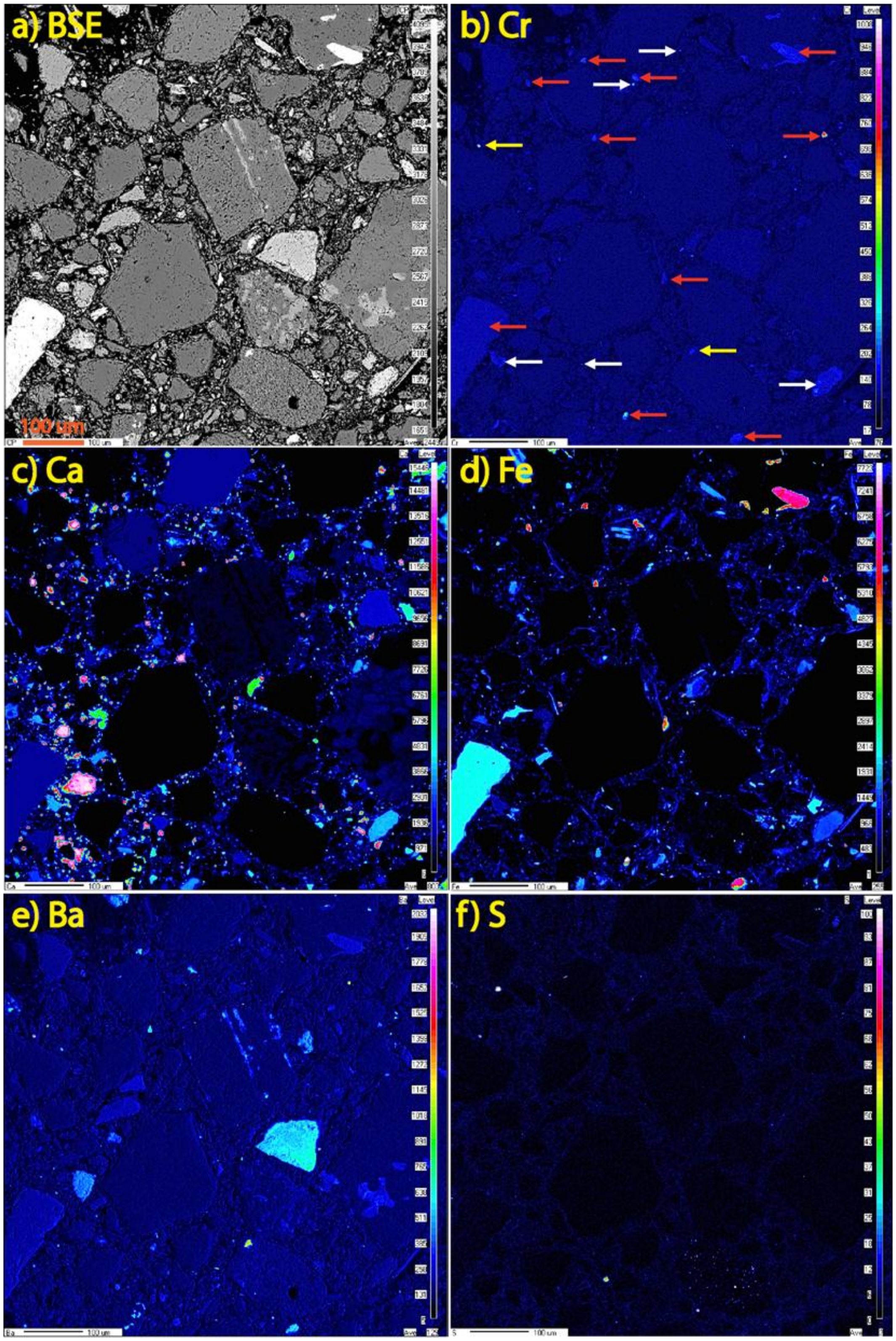

Figure 14. Element distribution of untreated (pre-leach) sediment 10: a) electron backscatter, b) Cr, c) Ca, d) Fe, e) Ba, and f) S. Arrows in (b) denote Cr association with Ca (white), Fe (red), and Ba (yellow).

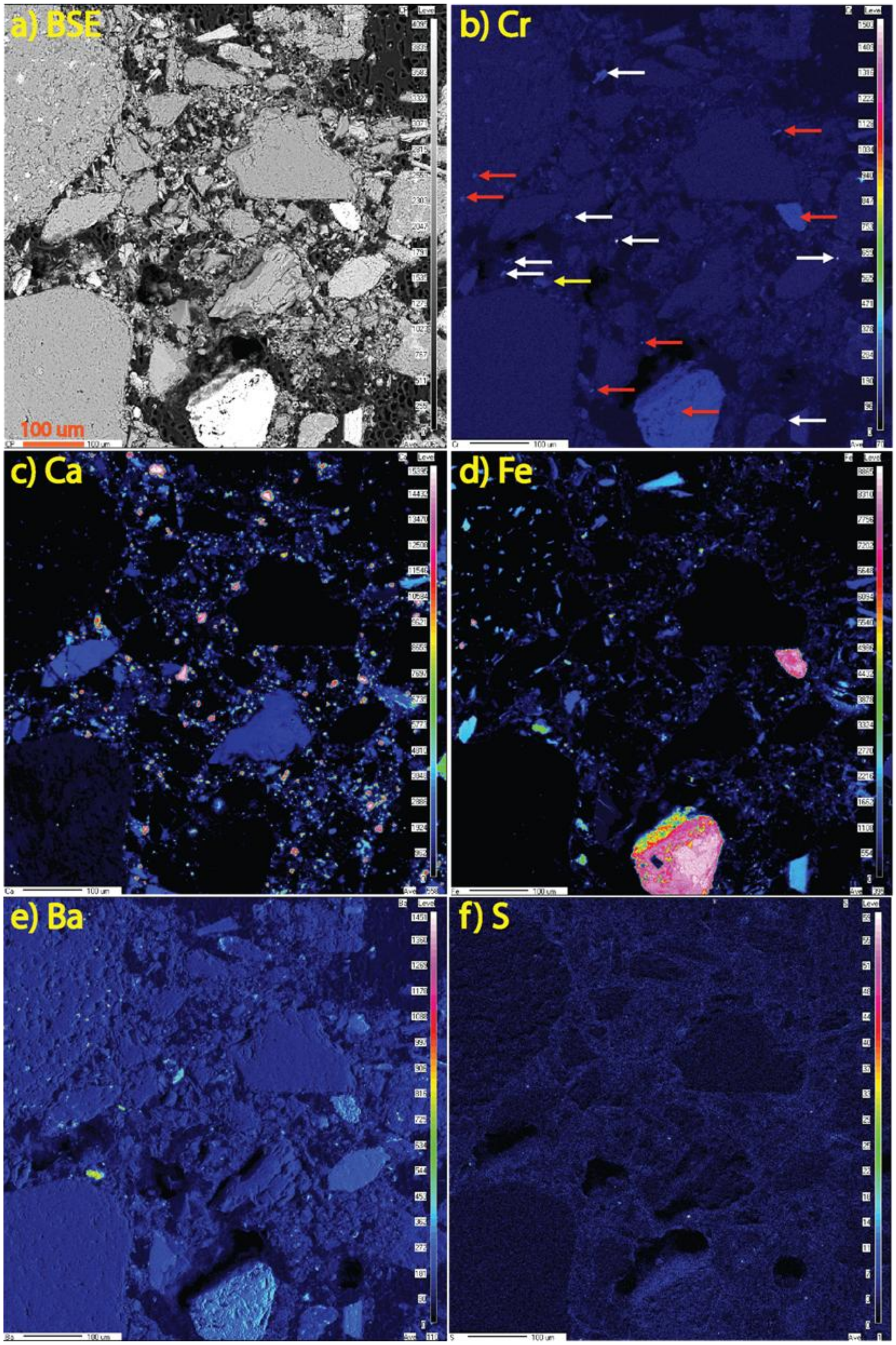

Figure 15. Element distribution of leached sediment 10: a) electron backscatter, b) Cr, c) Ca, d) Fe, e) Ba, and f) S. Arrows in (b) denote Cr association with Ca (white), Fe (red), and Ba (yellow).

Additional evidence and information were collected about Cr(VI) co-precipitation with calcium carbonate to assess its relevance to attenuation away from source areas. These results extend the data about Cr(VI) co-precipitation from the literature (e.g., Tang et al. 2007; Hua et al. 2007) to lower starting aqueous-phase Cr(VI) concentrations. The experiment conducted with a 44 ppb Cr(VI) solution showed that more than 86% of the aqueous Cr(VI) was removed from solution and likely incorporated into the calcium carbonate precipitates (Table 4). At higher initial Cr(VI) concentrations, a lower percentage of the supernatant concentration (13−27%), but greater total mass of Cr(VI), was incorporated into the calcium carbonate precipitate. These data showed that even at low initial Cr(VI) concentrations, a substantial amount of Cr(VI) can co-precipitate with calcium carbonate and this mechanism may be relevant for Cr(VI) concentrations within the plume, not just at a source area (though it could be strongest in a source area due to perturbed geochemical conditions).

Table 4. Calculated Cr(VI) uptake in calcium carbonate minerals and the percent aqueous Cr(VI) removed from solution at different initial Cr(VI) concentrations.

Initial Aqueous-Phase Cr(VI) Concentration	Cr(VI) Content in the Precipitate (μg/g)[a] (4-hour contact time)	% Cr(VI) Removed from Solution (4-hour contact time)
44 ppb	0.8	87[b]
1 ppm	5.4	27
5 ppm	18	18
30 ppm	76	13
100 ppm	130	6.9

(a) Assuming the mass of precipitated calcium carbonate was similar regardless of the initial Cr(VI) concentration in solution.

(b) Calculated assuming the supernatant Cr(VI) concentration was equal to the 6-μg/L analytical detection limit.

XRD results revealed the presence of both vaterite and calcite in the solid precipitates formed during the co-precipitation experiments. Vaterite and calcite are different solid-state phases of calcium carbonate that have a different morphology (Figure 16). Calcite was the dominant precipitated solid phase in most experiments. Tang et al. (2007) showed calcite as the precipitate formed during Cr(VI) co-precipitation in calcium carbonate solutions. However, in the experiment with the 100 ppm initial aqueous-phase Cr(VI) concentration, over 70% of the precipitate was observed to be vaterite. Some researchers have shown precipitation of calcium carbonate by mixing concentrated Ca^{2+} and CO_3^{2-} solutions involving at least three steps: formation of amorphous calcium carbonate, transformation of amorphous calcium carbonate into vaterite and calcite, and transformation of the thermodynamically unstable vaterite into stable calcite (Wei et al. 2003; Shen et al. 2006; Hua et al. 2007). Importantly, the mechanism of the last step is considered to be a dissolution and recrystallization of the unstable vaterite into stable calcite (Shen et al. 2006; Wei et al. 2003). In addition, the transformation of vaterite to calcite is usually spontaneous and can be readily triggered by merely contact with water (Hua et al. 2007). Therefore, some or all of the precipitated Cr(VI) in a vaterite solid phase may be released back into solution during solid-phase transformation reactions from amorphous calcium carbonate and/or vaterite to more stable calcite. Further research would be needed to evaluate vaterite precipitation and quantify the process of vaterite transformation to calcite in terms of rate and extent of Cr(VI) release after precipitation. In the co-precipitation experiments for this study (Table 4), Cr(VI) supernatant concentrations measured over a period of 72 hours showed potential minor increases except for an increase observed in the 1 ppm Cr(VI) treatment (Figure 17). An increase in the supernatant concentration would indicate dissolution of a Cr(VI) precipitate. During this time, the pH increased, but remained within one pH unit of variation (1, 5, and 30 ppm treatments) and two pH units (100 ppm treatment).

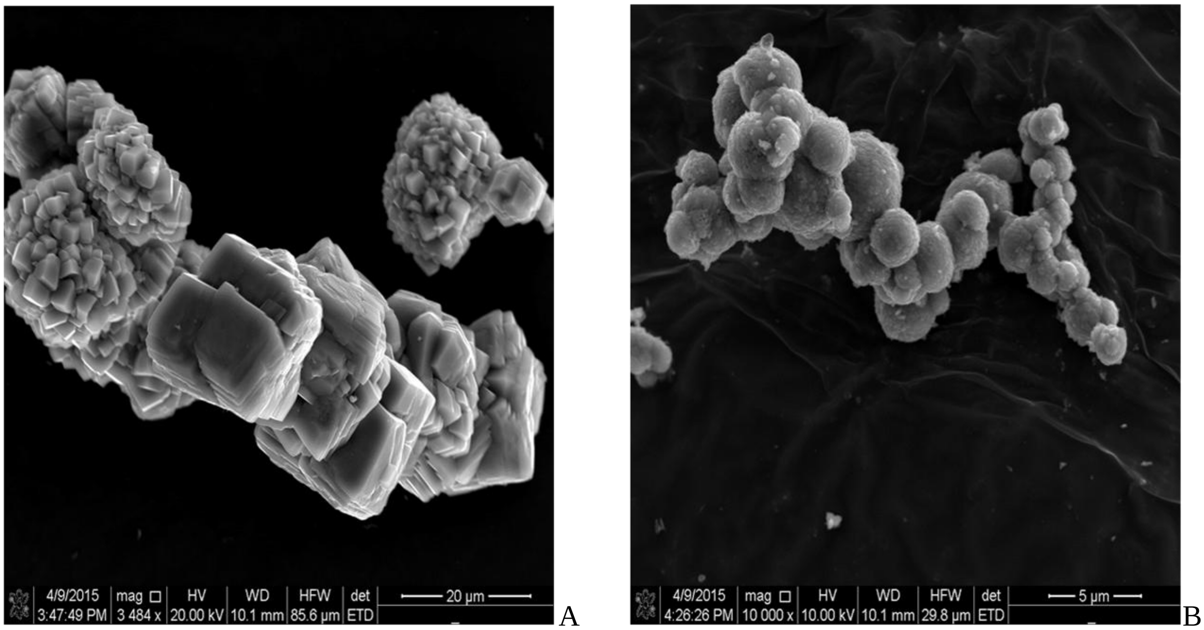

Figure 16. Scanning electron microscope images of precipitates formed in co-precipitate experiments showing the morphology of A) calcite (from an experiment with no added Cr(VI)) and B) vaterite (from the experiment with 100 ppm Cr(VI) added).

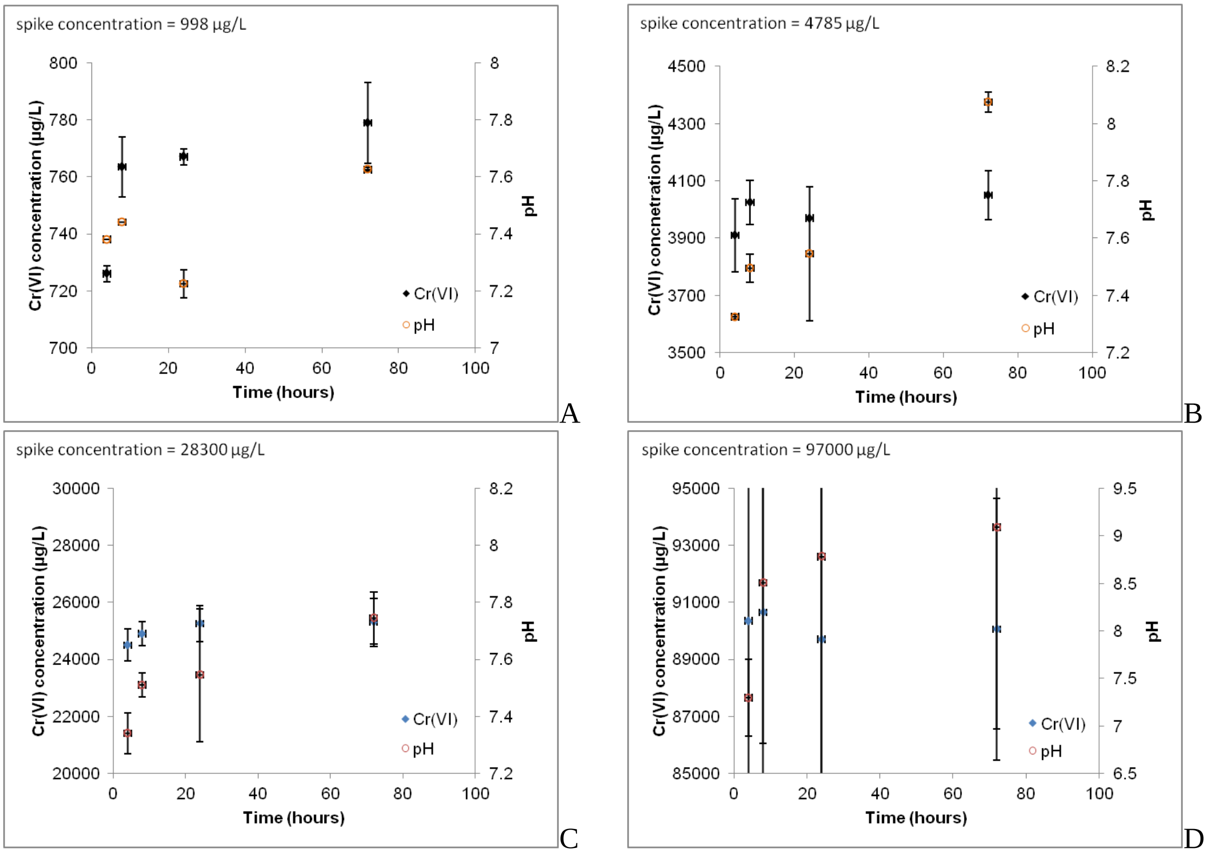

Figure 17. Supernatant Cr(VI) concentration and pH in the of co-precipitation experiments for nominal spike concentrations of A) 1 ppm, B) 5 ppm, C) 30 ppm, and D) 100 ppm. The Cr(VI) concentrations in the treatment spiked with 44 µg/L were all below the 6 µg/L analytical detection limit during this time.

4.0 Implications for the Hanford 100 Area

This section discusses interpretation of the laboratory results for application to 100 Area Cr(VI) plume behavior and for use in MNA evaluations.

4.1 Relevance of Laboratory Results to 100 Area Cr(VI) Plumes

Although the aquifer in the Hanford 100 Areas generally contains dissolved oxygen (i.e., is oxic), sediments retrieved from the aquifer showed the ability to reduce Cr(VI). With any type of sampling, sediment structure is disturbed. Thus, some of the reductive capacity may be due to this disturbance, creating fresh sediment surfaces that have reductive capacity (e.g., through breaking of sediment particles or abrasion of sediment particle surfaces). However, collected sediments were only partially saturated and were stored for months under atmospheric conditions. During this time, there was an opportunity for any fresh surfaces to oxidize. Sediment samples for experiments were also sieved and the <4 mm fraction was packed into soil columns for experiments. Through this sieving and repacking process, groundwater flow in the soil columns was more evenly distributed to contact all sediment materials, and the reductive capacity previously within isolated areas under aquifer sediment packing conditions may have been newly exposed to the bulk water system. For these reasons, the reductive capacity and rates observed in the laboratory tests may be higher than are present in the field.

While there are reasons for lower capacity and rates of Cr(VI) reduction under field conditions, the reductive capacity appears to be robust within the samples analyzed and, thus, may be occurring within parts of the aquifer. Chromium redox potential is high; it has a value somewhat lower than that of oxygen and near that of nitrate. Movement of chromium into lower permeability zones, where reductive capacity and lower dissolved oxygen concentrations may be present, may result in Cr(VI) reduction. Observing the effects of Cr(VI) reduction in the results of groundwater sample analysis from monitoring wells would be difficult for several reasons. Until recently, Cr(VI) sources were still feeding aquifer plumes and creating increasing/stable plumes. Under conditions where the source flux is much higher than the attenuation capacity, this type of attenuation would be masked by the added Cr(VI). For the Hanford 100-D, 100-H, and 100-K Areas, P&T-induced plume movement would tend to mask reductive attenuation, though reduction may be contributing to quicker decline of the plume than if it were not occurring.

Higher Cr(VI) reduction rates be expected within the finer-grained sediments because they likely contain a larger fraction of the relevant reactive facies. In addition, reduction would be greatest in lower permeability zones not readily accessed by groundwater samples collected from monitoring wells. Significant variations in chromium distribution have been observed in the detailed characterization conducted within the Ringold Formation beneath the 100-D-100 waste site in the 100-D Area (CHPRC 2015). This site contained Cr(VI) contamination throughout the vadose zone and into the underlying aquifer and exhibited persistently high Cr(VI) concentrations in groundwater prior to remediation. In borehole C8956, installed at the north end of the 100-D-100 excavation (Figure 18), analysis of sediment cores throughout the full depth of the aquifer showed non-detect results for Cr(VI) and measured total chromium concentrations of around 5−8 mg/kg. In nearby boreholes, Cr(VI) was present in discrete sediment samples, though concentrations varied significantly laterally (between boreholes) and vertically (e.g., between different layers in the Ringold Formation). Thus, even within a source zone, groundwater access to different sediment zones varies, as indicated by variations in sediment Cr(VI) concentrations.

The presence of variable amounts of total chromium may be related to variations in natural sediment chromium content or represent, in part, the result of some chromium reduction. For instance, borehole C8956 results may represent a zone where the total chromium concentrations are most representative of natural sediment-associated chromium (i.e., because of low contact with source-derived Cr(VI) contamination). Excluding samples of the aquitard (Ringold Mud unit) beneath the aquifer (which had high Cr(VI) and total chromium concentrations), the total chromium concentration in almost all of the samples from the other three boreholes (17 of 19 samples) was higher (up to three times higher) than that observed in borehole C8956. Cr(VI) was present in all of these other sediment samples.

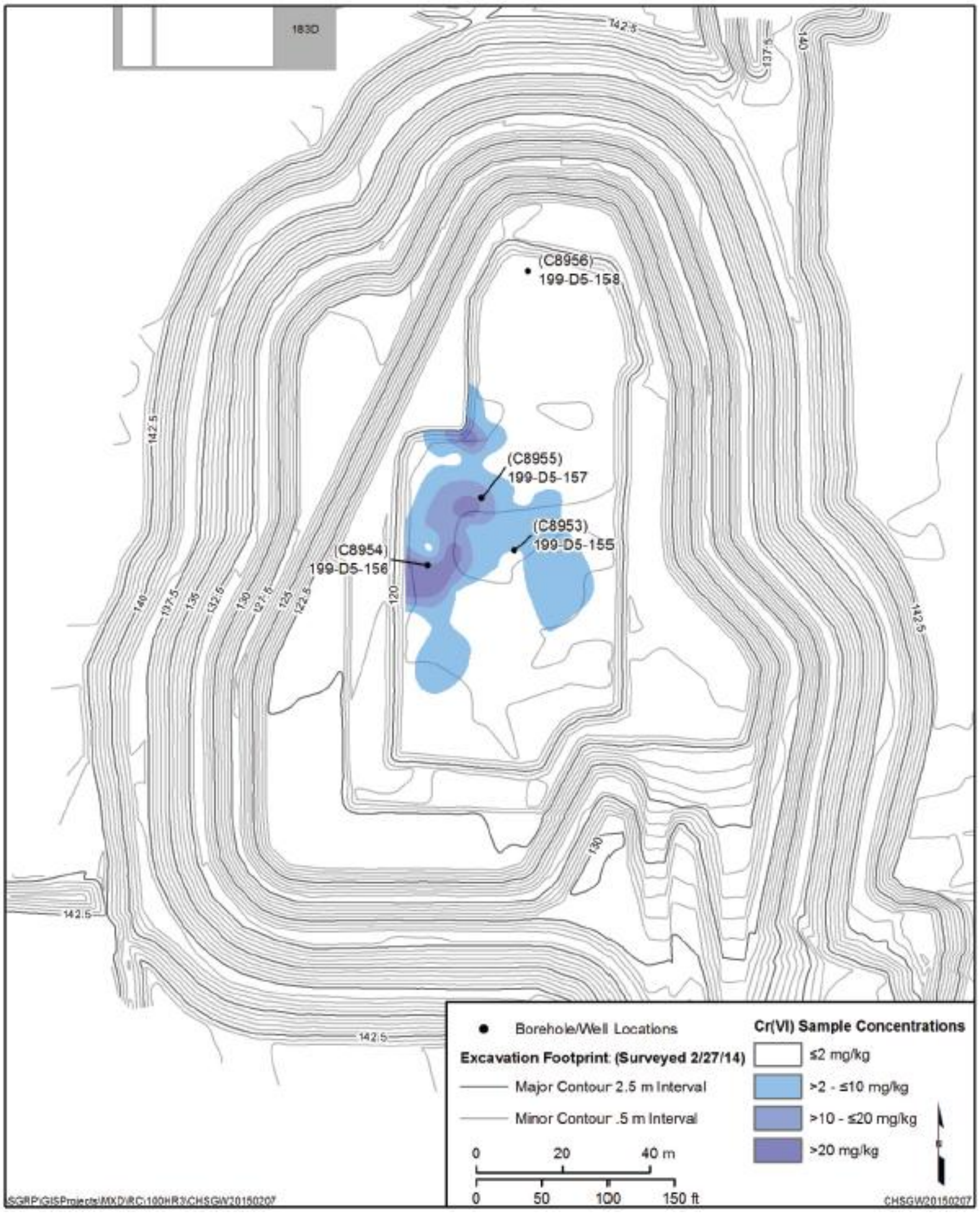

Figure 18. Borehole locations and inferred distribution of Cr(VI) in sediment at the water table for the 100-D-100 excavation (CHPRC 2015).

4.2 Implications for MNA Evaluations

Multiple lines of evidence are used in an MNA evaluation to demonstrate the presence of attenuation mechanisms and evaluate whether attenuation will be sufficient to meet RAOs. For the Hanford 100-D, 100-H, and 100-K Area Cr(VI) plumes, P&T operations have and are continuing to perturb the plume behavior (as designed) such that plume behavior cannot be directly used to assess natural attenuation rates. At these and other 100 Areas, plume conditions are in transition because source remediation actions were recently completed. Thus, monitoring well and plume trends must be interpreted in light of these declining or terminated source flux conditions. Where P&T has not been applied, direct monitoring over time may be suitable to demonstrate attenuation of plumes. For instance, plumes at the 100-F/IU and 100-BC Areas can be monitored in this way to support MNA evaluation. However, at these areas and other areas with some form of plume perturbation, predictive modeling is an important tool for evaluating MNA and its ability to meet RAOs. To support predictive modeling, a technical basis for selection of appropriate fate and transport parameters is needed to configure the model and to support interpretation of modeling results.

The information provided in this study describes attenuation mechanisms associated with 1) Cr(VI) reduction to functionally immobile Cr(III) that acts as a loss mechanism (e.g., like degradation), 2) co-precipitation of Cr(VI) with calcium carbonate materials of moderate solubility that act as a solubility-controlled partitioning interaction with respect to slowing Cr(VI) transport (e.g., within the plume especially at the distal portions), and 3) co-precipitation of Cr(VI) with calcium carbonate materials of moderate solubility that may provide a continuing source of Cr(VI) (e.g., for the tail of a plume or near former source areas). These mechanisms are important to incorporate into MNA evaluations. Low-solubility Cr(VI) compounds such as barium chromate ($BaCrO_4$) were also observed in sediment samples and were stable with respect to leaching. Formation of low-solubility compounds may be a potential loss mechanism, but is less likely to be prevalent throughout the plume, as may occur with co-precipitation of Cr(VI) with calcium carbonate.

The Cr(VI) reduction observed in the laboratory is expected to be difficult to directly observe in the field because 1) it may be masked by Cr(VI) concentrations and transport in higher permeability zone that are preferentially sampled by monitoring wells and 2) sediment samples collected at locations further from the source areas would be expected to have low concentrations of Cr(VI) and Cr(III). Cr(VI) reduction is expected to be most active in fine-texture lower permeability zones where reactive facies such as reduced iron and microbial populations are higher, and dissolved oxygen concentrations are more likely to be lower. However, because Cr(VI) has been observed to be robust in the 100 Area sediments included in this study, it is reasonable to consider reduction as one of the attenuation mechanisms that can be attributed to declining plume conditions. Thus, if data demonstrate plume decline, this plume decline could be attributed to dispersion, sorption, and reductive processes. If a model is used to evaluate plume behavior and predict future plume behavior, inclusion of a reduction rate that helps match observed plume dynamics may be appropriate using the data from this study as a technical basis to include a reduction process. For these purposes, a reduction rate that is slower than observed in the laboratory tests would be most likely relevant for use as a field-scale rate. It would also be more appropriate to apply this reduction rate to the Ringold Formation or Ringold/fine-texture inclusions (i.e., rip-up clasts) within the Hanford formation. Monitoring observations for the 100-F/IU and 100-BC Areas may provide important data to examine plume decline and the contributions to attenuation by dispersion, sorption, and reductive processes.

The laboratory results show that there is some finite capacity for Cr(VI) reduction. This capacity would be expected to vary in the aquifer, but be highest in the fine-textured zones. Depending on sediment conditions and the flux of Cr(VI) and other electron acceptors into a sediment zone, this capacity would eventually be reached and the reductive attenuation process would no longer be operable. This capacity would be more likely to have been reached for the plume core zones than at the plume periphery. Based on the study results, Cr(VI) reductive activity appears to be from a combination of biotic and abiotic processes. Biotic activity, if there is a source of electron donor to feed the reactions, can sustain and increase reductive capacity through direct Cr(VI) reduction or through indirectly creating reduced sediment minerals that can reduce Cr(VI). Facultative microorganisms, those microorganisms that can utilize dissolved oxygen or anaerobic electron acceptors (e.g., Cr(VI) or Fe(III)), are capable of this type of activity. It appears that dissolved oxygen suppresses the reductive activity, but does not eliminate it. The ferrous iron content in sediment samples prior to testing was about one-third of the total iron content. Thus, reduced iron is present in the sediment even in an oxic aquifer, as has been observed for other investigations. For instance, data from the 200 Area suggest that ferrous iron concentrations in Ringold materials could be on the order of 3.4 to 6.9 wt% (MinChem Database – unpublished). Potentially, some of these ferrous phases can reduce Cr(VI), but they are less active with dissolved oxygen and therefore not converted to ferric iron by dissolved oxygen. In evaluating future plume behavior, available reductive capacity at the distal portions of the plume and within finer-textured sediment features would be most appropriate to consider. Laboratory results provided a rough estimate of the capacity that could be used to constrain the reductive attenuation element of an attenuation assessment.

Co-precipitation of Cr(VI) with calcium carbonate materials has several implications. Source zone implications of the co-precipitated Cr(VI) were evaluated in a recent field investigation report (CHPRC 2015). At this site, high Cr(VI) concentrations have sustained a Cr(VI) plume for decades. Release of Cr(VI) from the vadose zone was initially identified as the likely source based on a conceptual model that considers Cr(VI) a mobile contaminant. However, the finding of elevated sediment-associated Cr(VI) in the periodically rewetted zone and aquifer beneath the vadose zone source area demonstrated that dissolution of solid-phase Cr(VI) precipitates can contribute to a continuing source. Sustained leaching of Cr(VI) from these sediments was demonstrated in laboratory soil column tests and provided kinetic data to quantify release rates in a way that can be implemented for modeling this type of source term (CHPRC 2015). This type of co-precipitation process may also occur throughout the plume. As shown herein, co-precipitation occurs at Cr(VI) concentrations at least as low as 44 µg/L (below the drinking-water standard). Thus, within the plume some Cr(VI) plume retardation may occur due to this process. The information in this report provides a basis for considering "sorptive" attenuation through a solubility-controlled partitioning interaction, but additional efforts would be needed to quantify the Cr(VI) retardation factor related to the precipitation/dissolution processes.

5.0 References

Alam M, MA Hossain, DR Yonge, BM Peyton, and JN Petersen. 2006. "Bioreduction of Hexavalent Chromium in Flow-through Quartz Sand Columns." *Journal of Environmental Engineering-ASCE* 132(3):358–366.

Arnold RG, TJ Dichristina, and MR Hoffmann. 1988. "Reductive Dissolution of Fe(III) Oxides by Pseudomonas Sp 200." *Biotechnology and Bioengineering* 32(9):1081–1096.

Bidoglio G, PN Gibson, MO'Gorman, and KJ Roberts. 1993. "X-ray absorption spectroscopy investigation of surface redox transformations of thallium and chromium on colloidal mineral oxides," *Geochimica et Cosmochimica Acta* 57(10):2389–2394.

Bopp LH and HL Ehrlich. 1988. "Chromate Resistance and Reduction in Pseudomonas-Fluorescens Strain Lb300." *Archives of Microbiology* 150(5):426–431.

Caccavo F, RP Blakemore, and DR Lovley. 1992. "A Hydrogen-Oxidizing, Fe(III)-Reducing Microorganism from the Great Bay Estuary, New-Hampshire." *Applied and Environmental Microbiology* 58(10):3211–3216.

CHPRC. 2015. *Persistent Source Investigation at 100-D Area*. Rev. 1, SGW-58416, CH2M Hill Plateau Remediation Company, Richland, Washington.

Coleman ML, DB Hedrick, DR Lovley, DC White, and K Pye. 1993. "Reduction of Fe(III) in Sediments by Sulfate-Reducing Bacteria." *Nature* 361(6411):436–438.

Davis JA and JO Leckie. 1980. "Surface Ionization and Complexation at the Oxide/Water Interface. III. Adsorption of Anions." *Journal of Colloid and Interface Science* 74(1):32–43.

Deng B and AT Stone. 1996a. "Surface-catalyzed Cr(VI) reduction: the TiO2-Cr(VI)-mandelic acid system." *Environmental Science and Technology* 30:463–472.

Deng B and AT Stone. 1996b. Surface-catalyzed Cr(VI) reduction: reactivity of different organic reductants and different oxide surfaces. *Environmental Science and Technology* 30:2484–2494.

DiChristina TJ. 1994. "Bioextraction (Reductive Dissolution) of Iron from Low-Grade Iron-Ores – Fundamental and Applied Studies." *Annals of the New York Academy of Sciences* 721:440–449.

Dresel PE, NP Qafoku, JP McKinley, JS Fruchter, CC Ainsworth, C Liu, ES Ilton, and JL Phillips. 2008. *Geochemical Characterization of Chromate Contamination in the 100 Area Vadose Zone at the Hanford Site*. PNNL-17674, Pacific Northwest National Laboratory, Richland, Washington.

Eary LE and D Rai. 1987. "Kinetics of chromium(III) oxidation to chromium(VI) by reaction with manganese dioxide." *Environmental Science and Technology* 21(12):1187–1193.

Eary LE and D Rai. 1989. "Kinetics of Chromate Reduction by Ferrous Ions Derived from Hematite and Biotite at 25°C." *American Journal of Science* 289:180–213.

EPA (U.S. Environmental Protection Agency). 2007a. *Monitored Natural Attenuation of Inorganic Contaminants in Ground Water - Volume 1, Technical Basis for Assessment*. EPA/600/R-07/139, Washington, D.C.

EPA (U.S. Environmental Protection Agency). 2007b. *Monitored Natural Attenuation of Inorganic Contaminants in Ground Water - Volume 2, Assessment for Non-Radionuclides Including Arsenic, Cadmium, Chromium, Copper, Lead, Nickel, Nitrate, Perchlorate, and Selenium*. EPA/600/R-07/140, , Washington, D.C.

Fendorf SE and RJ Zasoski. 1992. "Chromium(III) Oxidation by Delta-Mno2. 1. Characterization." *Environmental Science and Technology* 26(1):79–85.

Fendorf SE, RJ Zasoski, and RG Burau. 1993. "Competing Metal-Ion Influences on Chromium(III) Oxidation by Birnessite." *Soil Science Society of America Journal* 57(6):1508–1515.

Fredrickson JK and YA Gorby. 1996. "Environmental Processes Mediated by Iron-Reducing Bacteria." *Current Opinion in Biotechnology* 7(3):287–294.

Gibbs CR. 1976. Characterization and application of ferrozine iron reagent as a ferrous iron indicator. *Analytical Chemistry Journal* 48(8):1197–1201.

Griffin RA, AK Au, and RR Frost. 1977. "Effect of pH on Adsorption of Chromium from Landfill-Leachate by Clay-Minerals." *Journal of Environmental Science and Health Part a -Environmental Science and Engineering & Toxic and Hazardous Substance Control* 12(8):431–449.

Horitsu H, S Futo, Y Miyazawa, S Ogai, and K Kawai. 1987. "Enzymatic Reduction of Hexavalent Chromium by Hexavalent Chromium Tolerant Pseudomonas-Ambigua G-1." *Agricultural and Biological Chemistry* 51(9):2417–2420.

Hua B, BL Deng, EC Thornton, J Yang, and JE Amonette. 2007. “Incorporation of chromate into calcium carbonate structure during coprecipitation.” *Water, Air and Soil Pollution* 179(1-4):381–390.

Ilton ES, DR Veblen, CO Moses, and SP Raeburn. 1997. “The catalytic effect of sodium and lithium ions on coupled sorption-reduction of chromate at the biotite edge-fluid interface.” *Geochimica et Cosmochimica Acta* 61(17):3543-3563.

Ishibashi Y, C Cervantes, and S Silver. 1990. “Chromium reduction in *Pseudomonas putida*”. *Applied and Environmental Microbiology* 56:2268–2270.

Kent DB, JA Davis, LCD Anderson, BA Rea, and TDWaite. 1994. “Transport of chromium and selenium in the suboxic zone of a shallow aquifer: Influence of redox and adsorption reactions.” *Water Resources Research* 30:1099–1114.

Kostka JE and KH Nealson. 1995. "Dissolution and Reduction of Magnetite by Bacteria." *Environmental Science and Technolology* 29(10):2535–2540.

Leckie JO, MM Benjamin, K Hayes, G Kaufman, and S Altman. 1980. *Adsorption/Coprecipitation of Trace Elements from Water with Iron Oxyhydroxides.* EPRI RP-910, Electric Power Research Institute, Palo Alto, California.

Lovley, D. R. 1991. "Dissimilatory Fe(III) and Mn(Iv) Reduction." *Microbiological Reviews* **55**(2):259-287.

Lovley DR and EJP Phillips. 1992. "Reduction of Uranium by Desulfovibrio-Desulfuricans." *Applied and Environmental Microbiology* 58(3):850–856.

Lovley DR and EJP Phillips. 1994. “Reduction of chromate by Desulfovibrio-vulgaris and its C(3) cytochrome.” *Applied and Environmental Microbiology* 60(2):726–728.

Lovley DR. 1994. Microbial Reduction of Iron, Manganese, and Other Metals. In *Advances in Agronomy*, Vol. 54. DL Sparks (ed), pp. 175–231, Academic Press, New York.

Namgung S, M Kwon, NP Qafoku, and GH Lee. 2014. "Cr(OH)3(s) Oxidation Induced by Surface Catalyzed Mn(II) Oxidation." *Environmental Science and Technology* 48(18):10760–10768. doi:10.1021/es503018u

Patterson RR and S Fendorf. 1997. "Reduction of hexavalent chromium by amorphous iron sulfide." *Environmental Science and Technology* 31(7):2039–2044.

Pflaum RT and LC Howick. 1956. The chromium-diphenylcarbazide reaction. *Proceedings of the American Chemical Society* 78:4862–2866.

Qafoku N, CC Ainsworth, JE Szecsody, O Qafoku, and SM Heald. 2003. "Effect of Coupled Dissolution and Redox Reactions on Cr(VI)(aq) Attenuation during Transport in the Sediments under Hyperalkaline conditions." *Environmental Science and Technology* 37(16):3640–3646.

Qafoku N, CC Ainsworth, and SM Heald. 2007. "Cr(VI) Fate in Mineralogically Altered Sediments by Hyperalkaline Waste Fluids." *Soil Science* 172(8):598–613.

Qafoku N, PE Dresel, JP McKinley, C Liu, SM Heald, CC Ainsworth, JL Phillips, and JS Fruchter. 2009. "Pathways of aqueous Cr(VI) attenuation in a slightly alkaline oxic subsurface." Environmental Science and Technology 43(4):1071-1077.

Qafoku N, PE Dresel, ES Ilton, JP McKinley, and CT Resch. 2010. "Chromium transport in an acidic waste contaminated subsurface medium: The role of reduction." *Chemosphere* 81(11):1492–1500. doi:10.1016/j.chemosphere.2010.08.043

Qafoku N, PE Dresel, JP McKinley, ES Ilton, W Um, CT Resch, RK Kukkadapu, and SW Petersen. 2011. *Geochemical Characterization of Chromate Contamination in the 100 Area Vadose Zone at the Hanford Site – Part 2*. PNNL-17865, Pacific Northwest National Laboratory, Richland, Washington.

Rai D, LE Eary, and JM Zachara. 1989. "Environmental chemistry of chromium." *Science of the Total Environment* 86(1-2):15–23.

Roden EE and JM Zachara. 1996. "Microbial Reduction of Crystalline Iron(III) Oxides: Influence of Oxide Surface Area and Potential for Cell Growth." *Environmental Science and Technology* 30(5):1618–1628.

Shen Q, H Wei, Y Zhou, Y Huang, H Yang, D Wang, et al. 2006. "Properties of amorphous calcium carbonate and template action of vaterite spheres." *Journal of Physical Chemistry B* 110:2994–3000.

Tang Y, EJ Elzinga, Y Jae Lee, and RJ Reeder. 2007. "Coprecipitation of chromate with calcite: Batch experiments and X-ray absorption spectroscopy." *Geochimica et Cosmochimica Acta* 71(6):1480–1493.

Wei H, Q Shen, Y Zhao, D Wang, and D Xu. 2003. "Influence of polyvinylpyrrolidone on the precipitation of calcium carbonate and on the transformation of vaterite to calcite." *Journal of Crystal Growth* 250:516–524.

White AF and ML Peterson. 1996. "Reduction of aqueous transition metal species on surfaces of Fe(II) containing oxides." *Geochimica et Cosmochimica Acta* 60(2):3799–3814.

Wittbrodt PR and CD Palmer. 1996. "Effect of temperature, ionic strength, background electrolytes, and Fe(III) on the reduction of hexavalent chromium by soil humic substances." *Environmental Science and Technology* 30(8):2470–2477.

Xie, Y, Murray, CJ, Last, GV, and R Mackley. 2003. *Mineralogical and Bulk-Rock Geochemical Signatures of Ringold And Hanford Formation Sediments*. PNNL-14202, Pacific Northwest National Laboratory, Richland, Washington.

Zachara JM, CC Ainsworth, CE Cowen, and CT Resch. 1989. "Adsorption of chromate by subsurface soil horizons." *Soil Science Society of America Journal* 53:418–428.

Zachara JM, CC Ainsworth, GE Brown, JG Catalano, JP McKinley, O Qafoku, SC Smith, JE Szecsody, SJ Traina, and JA Warner. 2004. "Chromium Speciation and Mobility in a High Level Nuclear Waste Vadose Zone Plume." *Geochimica et Cosmochimica Acta* 68(1):13–30.

Zhong L, NP Qafoku, JE Szecsody, PE Dresel, and ZF Zhang. 2009. "Foam Delivery of Calcium Polysulfide to Vadose Zone for Cr(VI) Immobilization – Laboratory Evaluation." *Vadose Zone Journal* 8(4). doi: 10.2136/vzj2008.0124.

Distribution

No. of Copies			No. of Copies		
2	**U.S. Department of Energy Richland Operations Office**			**Pacific Northwest National Laboratory**	
	JG Morse	(PDF)		MJ Truex	(PDF)
				JE Szecsody	(PDF)
				NP Qafoku	(PDF)
				BD Lee	(PDF)
				MH Lee	(PDF)
				DM Wellman	(PDF)

Pacific Northwest
NATIONAL LABORATORY

U.S. DEPARTMENT OF
ENERGY

Proudly Operated by **Battelle** *Since 1965*

902 Battelle Boulevard
P.O. Box 999
Richland, WA 99352
1-888-375-PNNL (7665)

www.pnnl.gov